
Simulating the earliest stages of heavy-ion collisions

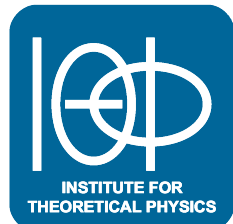
Teilchenphysikseminar Universität Wien
November 12, 2019

Andreas Ipp

based on

D. Gelfand, AI, D. Müller, Phys. Rev. D94 (2016) no.1, 014020
AI, D. Müller, Phys. Lett. B (2017) 771
AI, D. Müller, Eur.Phys.J. C78 (2018) no.11, 884

Institute for Theoretical Physics, TU Wien, Austria



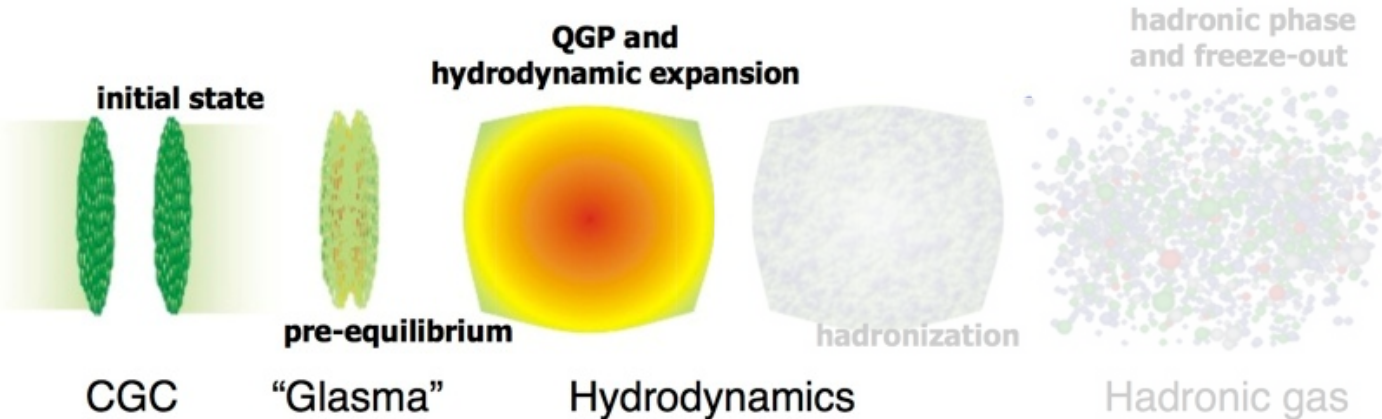
$\int dk \Pi$

FWF
Der Wissenschaftsfonds.



Outline

- Simulation of early stages of heavy-ion collisions
 - color-glass-condensate (CGC) framework
 - colored particle-in-cell (CPIC)
 - beyond boost-invariance
- Numerical results
 - energy density at different rapidities
 - comparison to RHIC data



Berndt Müller, arXiv:1309.7616

QCD phase diagram

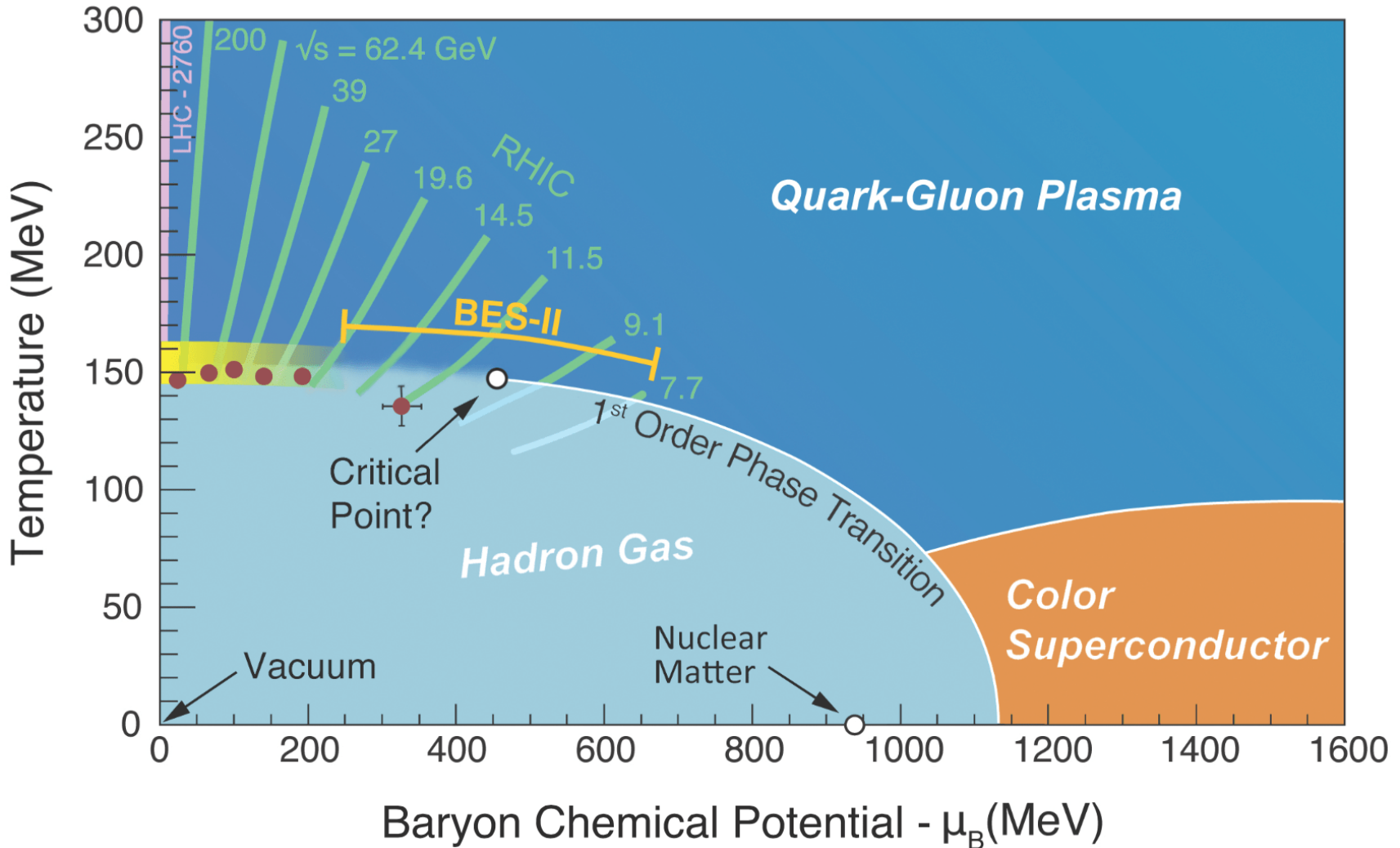
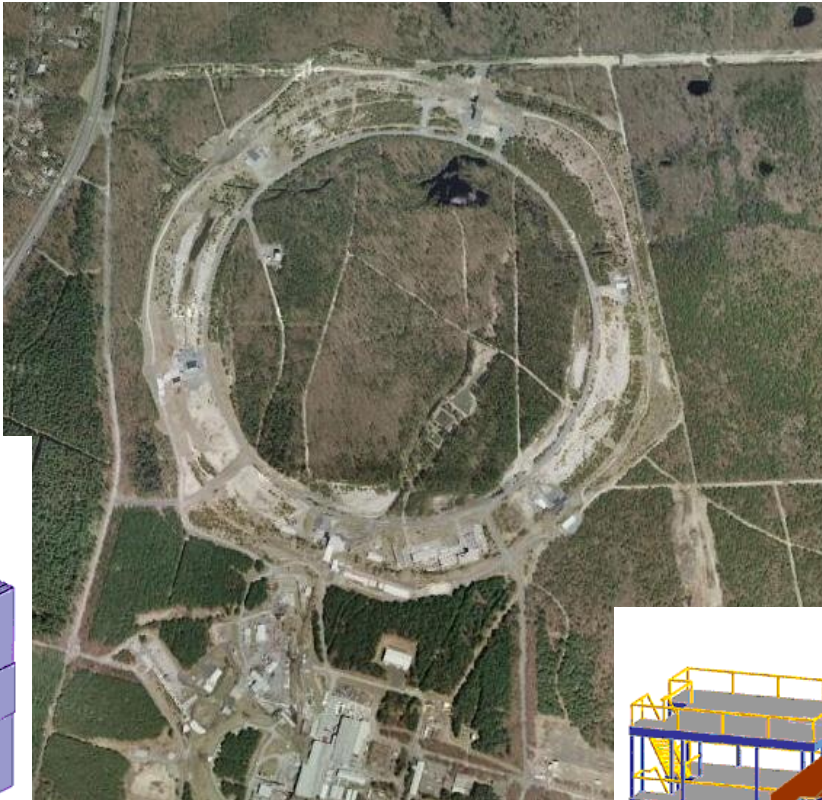
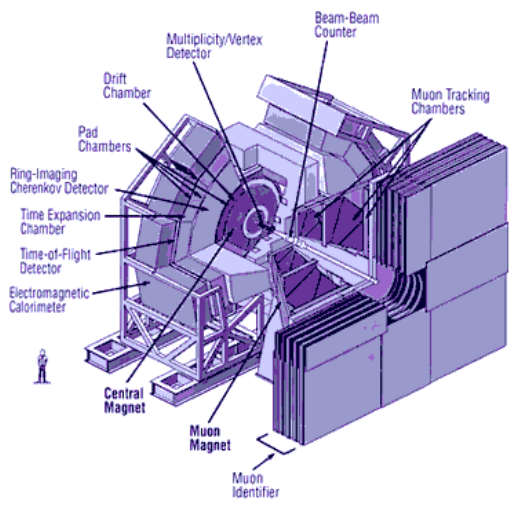


Illustration: Swagato Mukherjee, Brookhaven National Laboratory.

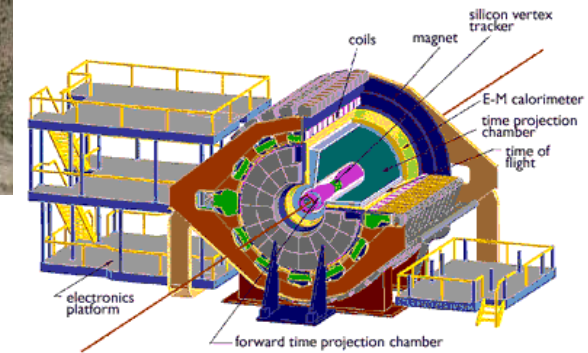
Relativistic Heavy Ion Collider (RHIC)

Brookhaven National Laboratory (USA)

PHENIX

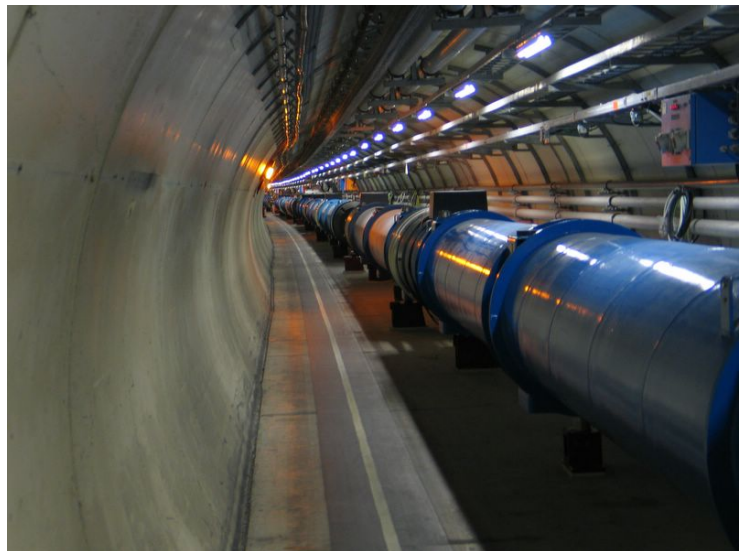
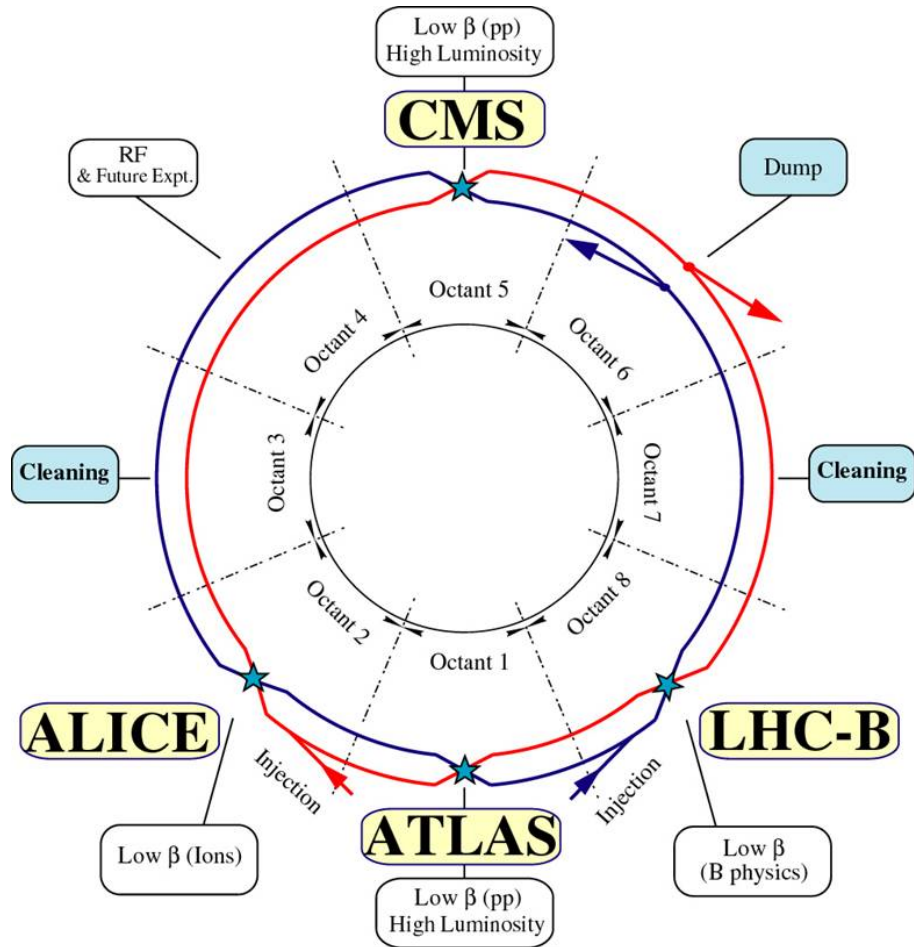


STAR

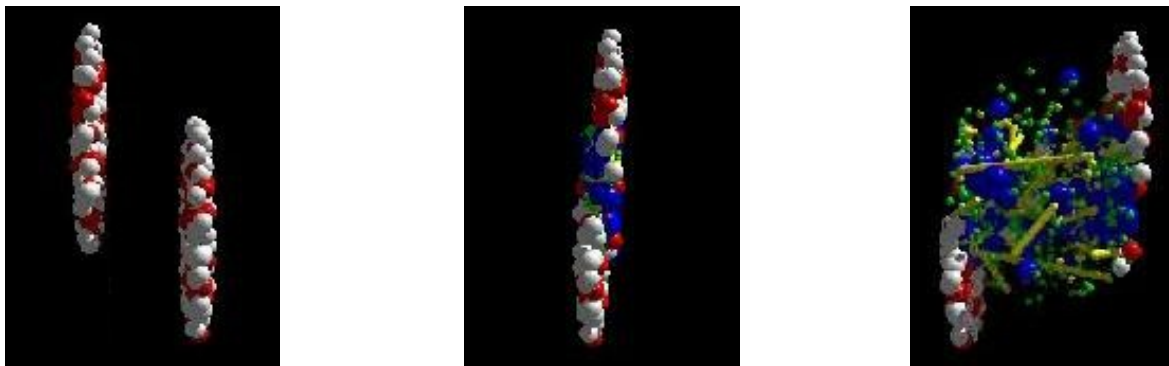


Large Hadron Collider (LHC)

CERN



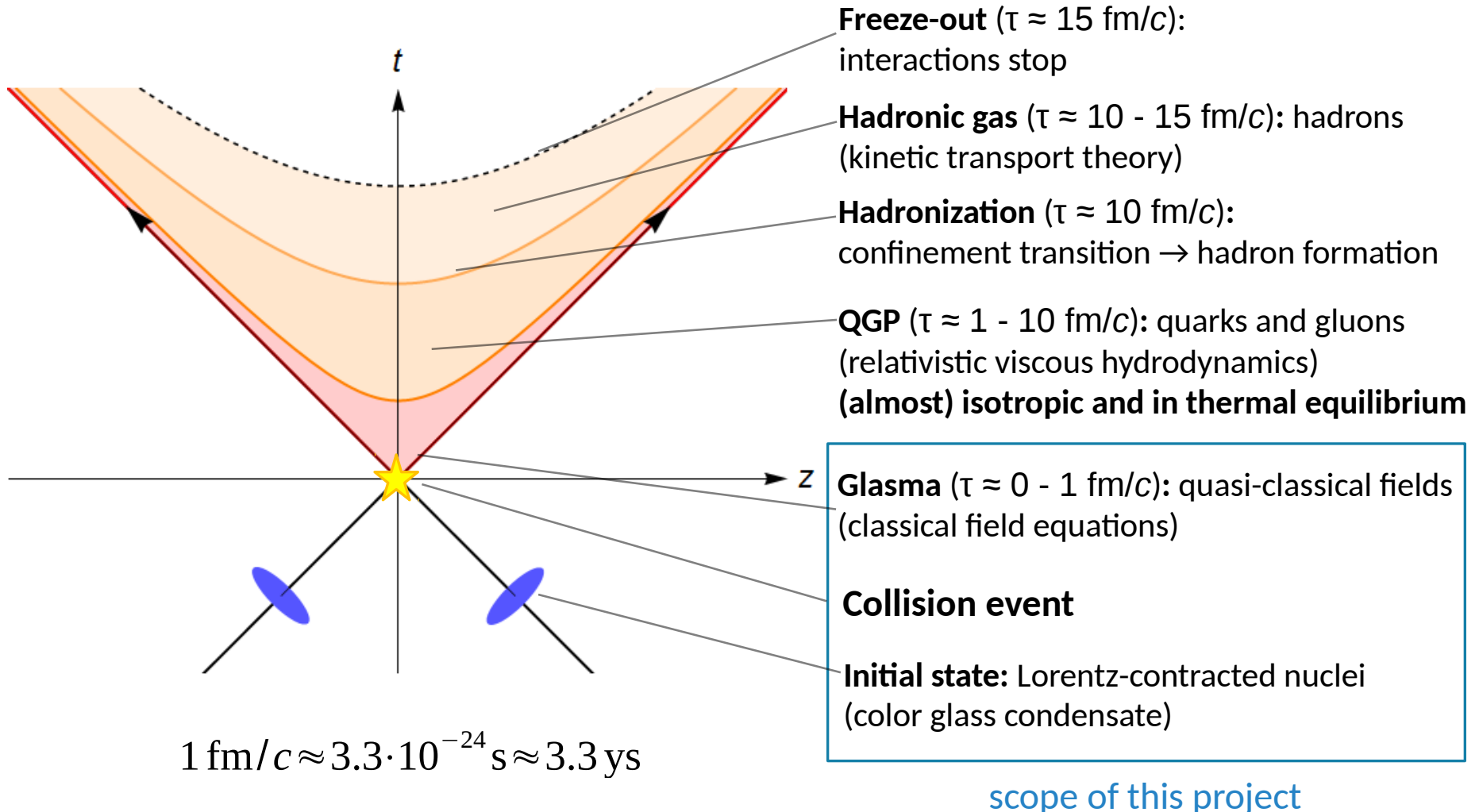
Heavy-ion collisions



(Simulation by UrQMD group, Frankfurt)

- Heavy ion nuclei (gold, lead) ($d \sim 14$ fm)
- formation time of QGP: $t \sim 1$ fm/c ≈ 3 ys
- QGP phase: RHIC 15 ys, LHC 25 ys
- good agreement with hydrodynamic simulations

Stages of a heavy-ion collision



Pancake thickness

French crêpe



© Image: David Monniaux

LHC (ALICE) @ CERN: Pb+Pb
with **~5.5 TeV** per nucleon pair
($\gamma \approx 2700$)

American pancake



RHIC @ BNL: Au+Au
with **~200 GeV** ($\gamma \approx 100$)

RHIC beam energy scan:
~7.7 – 62.4 GeV ($\gamma \approx 4 - 30$)

Color glass condensate

Nuclei at ultrarelativistic speeds can be described by **classical effective theory** in the color glass condensate (CGC) framework.

[Gelis, Iancu, Jalilian-Marian, Venugopalan, Ann.Rev.Nucl.Part.Sci.60:463-489,2010]

Large gluon occupation numbers → coherent, classical gluon field

Split degrees of freedom into ...

- Hard partons = classical color charges  generates..
- Soft gluons = classical gauge field
- Static field configuration due to time dilation.
- Collision of two such classical fields creates the **Glasma**.

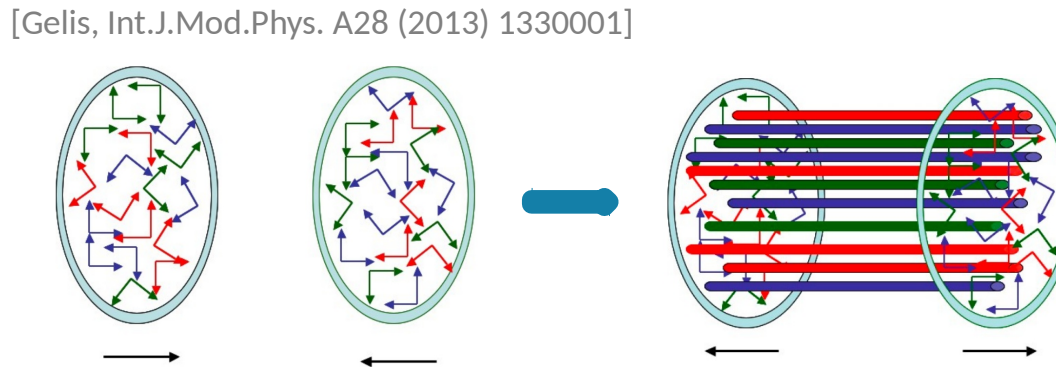
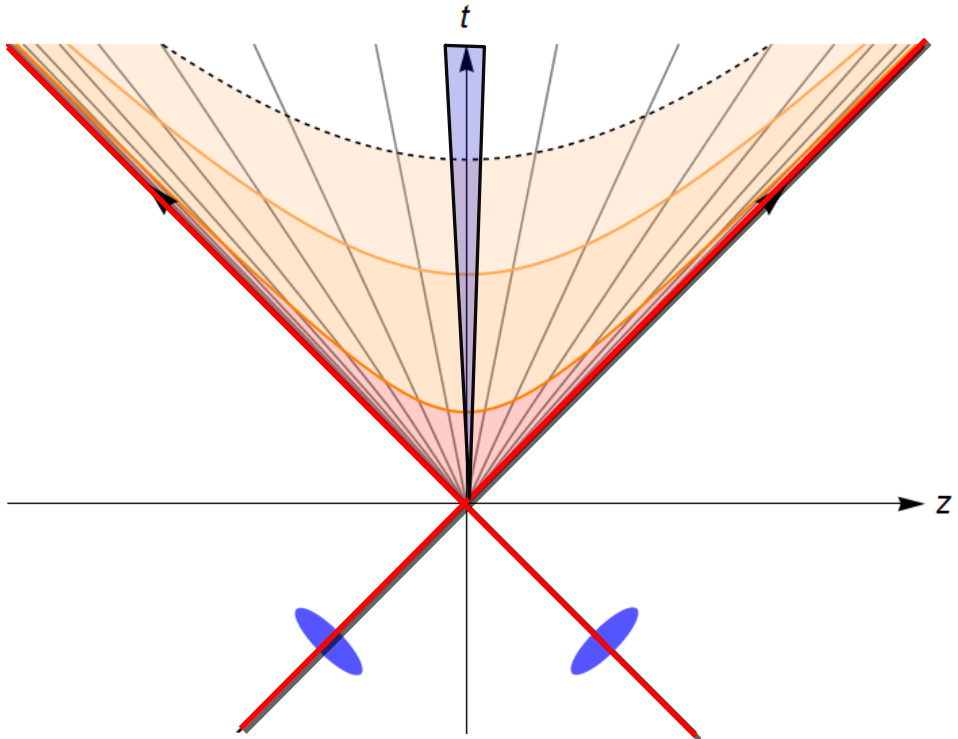


Figure from L. McLerran:
Proceedings of ISMD08, p.3-18 (2008)

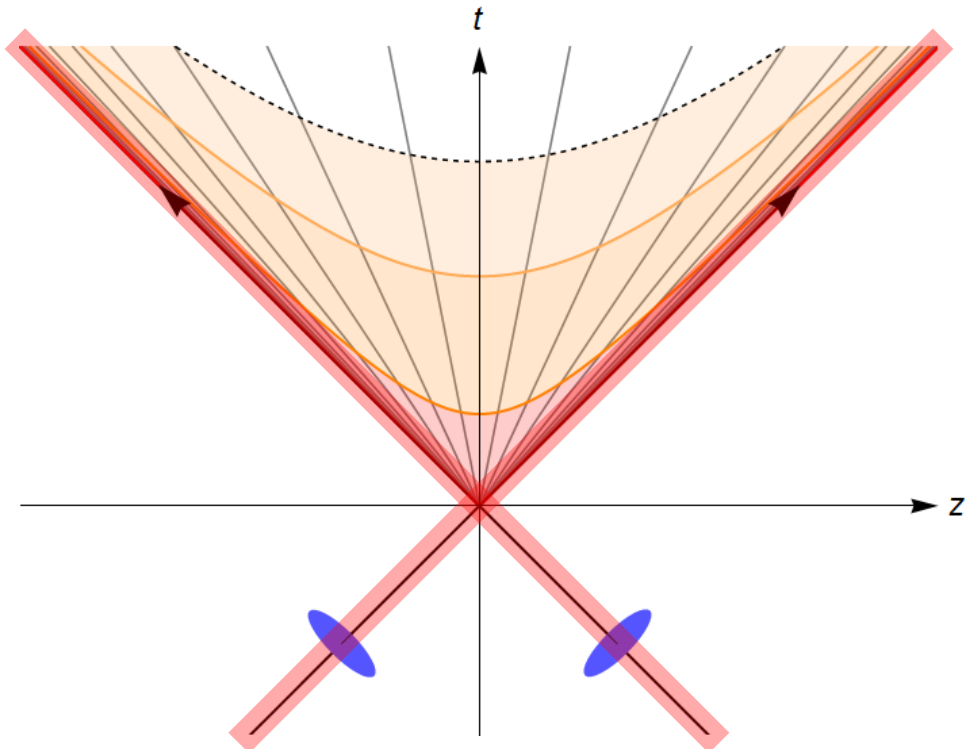
Boost-invariant CGC collision



- color glass condensate (CGC): hard and soft degrees of freedom, weak coupling
- infinitely thin color currents
- boost-invariant solution
- solve Yang-Mills equations numerically in 2+1 D

$$D_\mu F^{\mu\nu}(\tau, x_T) = 0$$

Finite nucleus thickness



- extended color currents
- boost-invariance lost
- solve full 3+1 D Yang-Mills equation with currents

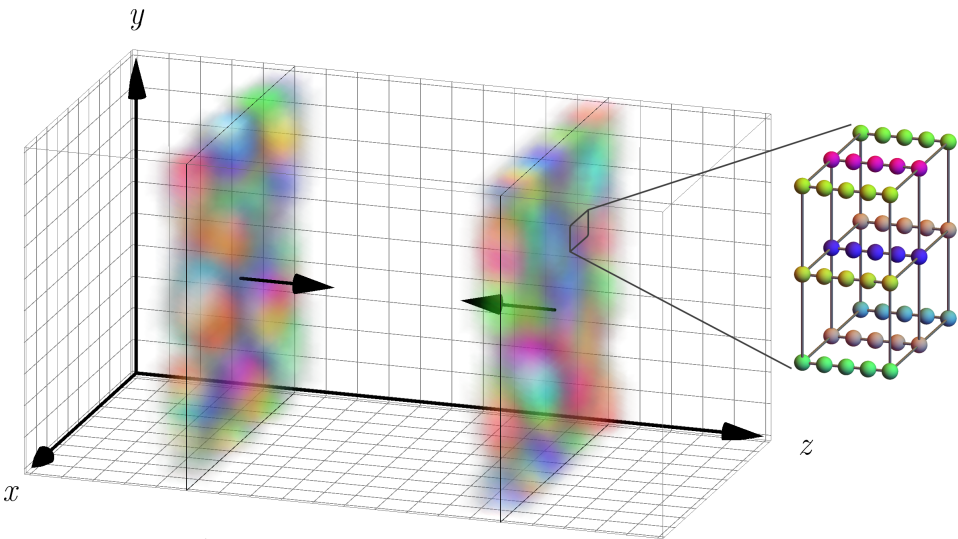
$$D_\mu F^{\mu\nu}(t, z, x_T) = J_1^\nu + J_2^\nu$$

$$D_\mu J^\mu(t, z, x_T) = 0$$

$$D_\mu \equiv \partial_\mu + ig [A_\mu, \cdot]$$

→ use Colored particle-in-cell (CPIC)
in laboratory frame

Colored particle-in-cell (CPIC)



CPIC: non-Abelian generalization of the particle-in-cell method from plasma physics.

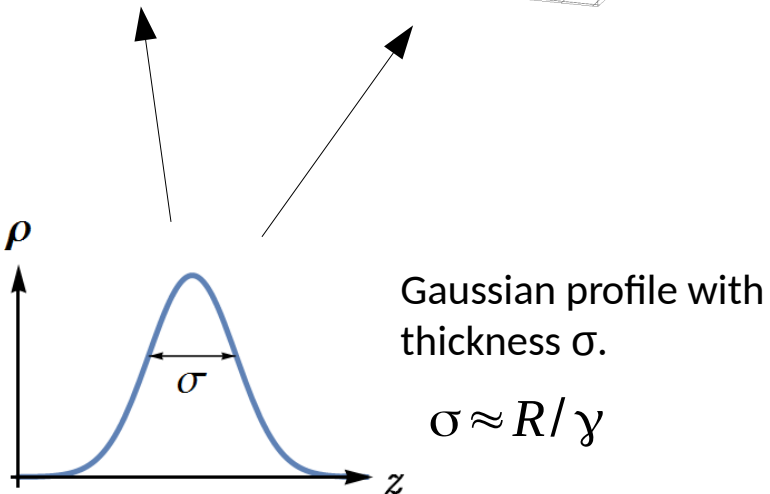
[A. Dumitru, Y. Nara, M. Strickland: PRD75:025016 (2007)]

Nucleus model: 2D McLerran-Venugopalan (MV) model

[McLerran, Venugopalan: PRD49 (1994) 3352-3355]

$$\langle \hat{\rho}^a(\mathbf{x}_T) \hat{\rho}^b(\mathbf{x}'_T) \rangle = g^2 \mu^2 \delta^{(2)}(\mathbf{x}_T - \mathbf{x}'_T) \delta^{ab}$$

$$\mu \approx 0.5 \text{ GeV} \quad (\text{Au, RHIC})$$

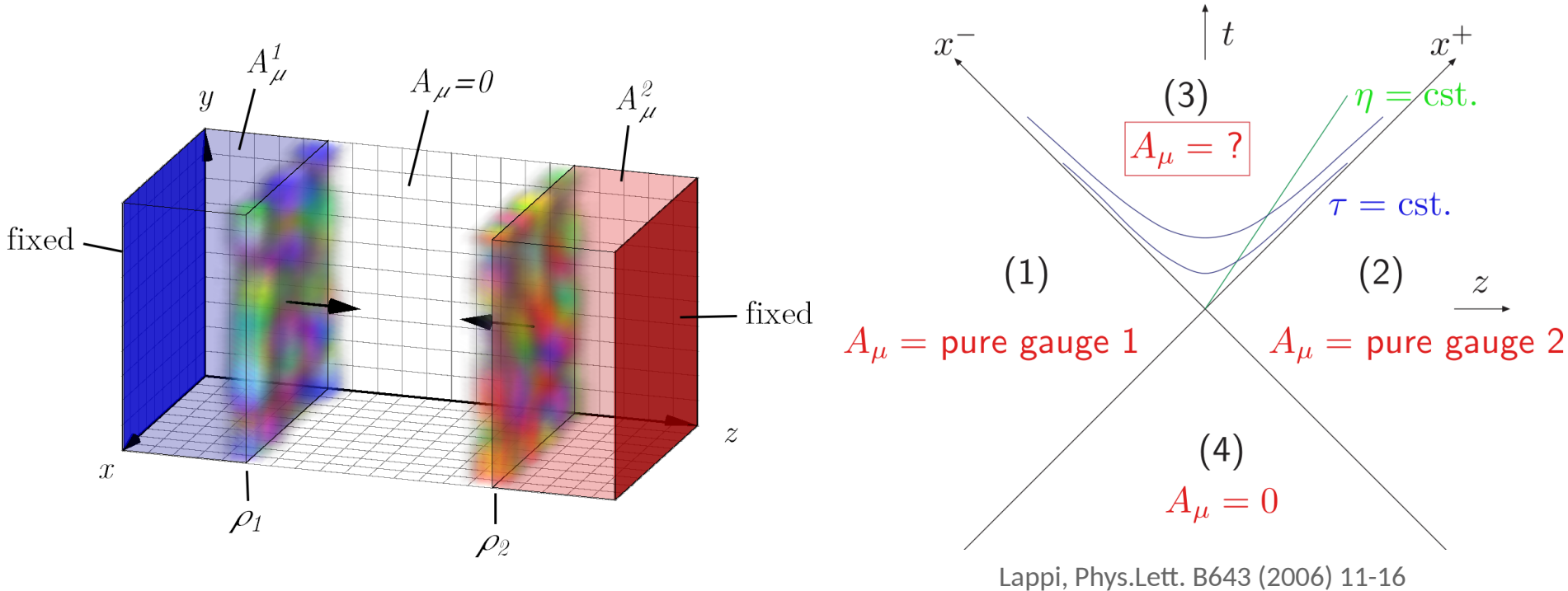


(no random longitudinal structure)

Infrared regulation

$$m \approx 200 \text{ MeV}$$

Implementation



Continuum equations of motion

$$D_\mu^{ab} F^{b,\mu\nu} = j^{a,\nu}$$

Lattice equations of motion

$$\dot{E}_i^a(x) = \frac{2}{ga^3} \sum_{j \neq i} \text{Im} [\text{tr} (U_{ij}(x) + U_{i-j}(x))] - j_i^a(x)$$

$$U_{ij}(x) = U_i(x)U_j(x+i)U_{-i}(x+i+j)U_{-j}(x+j)$$

$$\dot{U}_i(x) = -iga E_i^a(x) t^a U_i(x)$$

Parallel transporters (gauge links): $U_i(x) = \exp(iga A_i^a(x) t^a)$

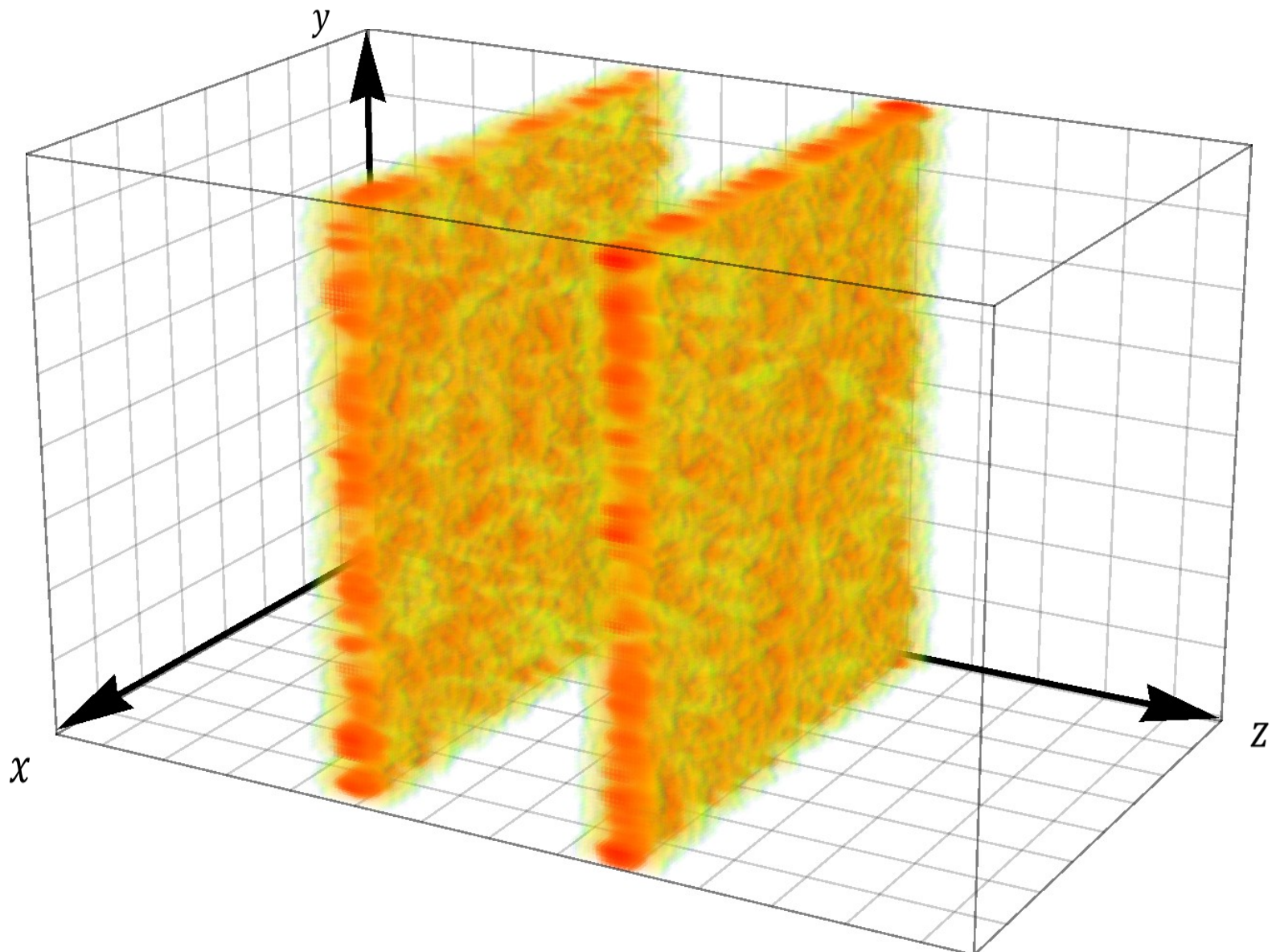
Results

Austrian Kaiserschmarrn („Emperor's mess“)

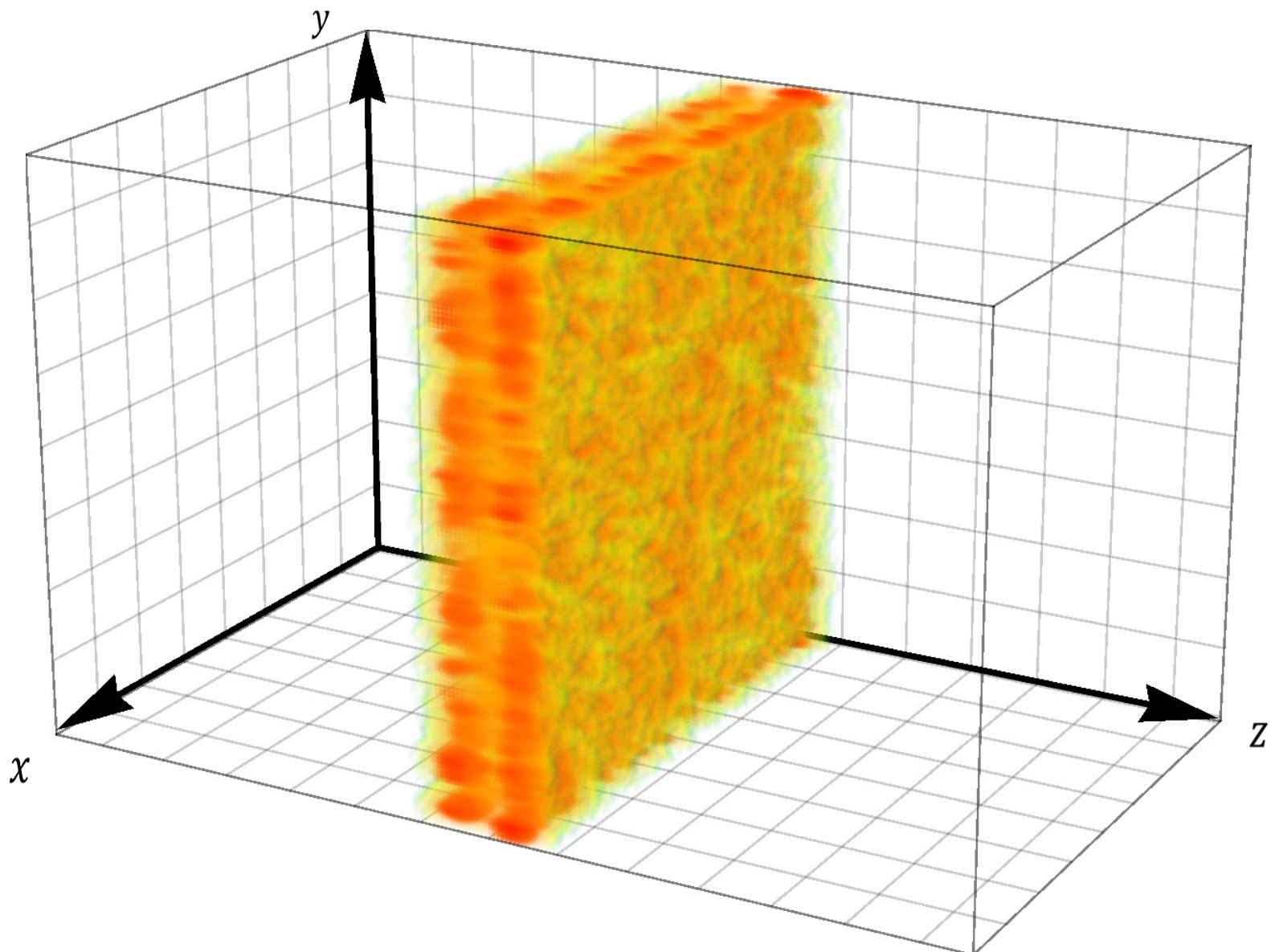


© Image: Aleksi Pihkanen

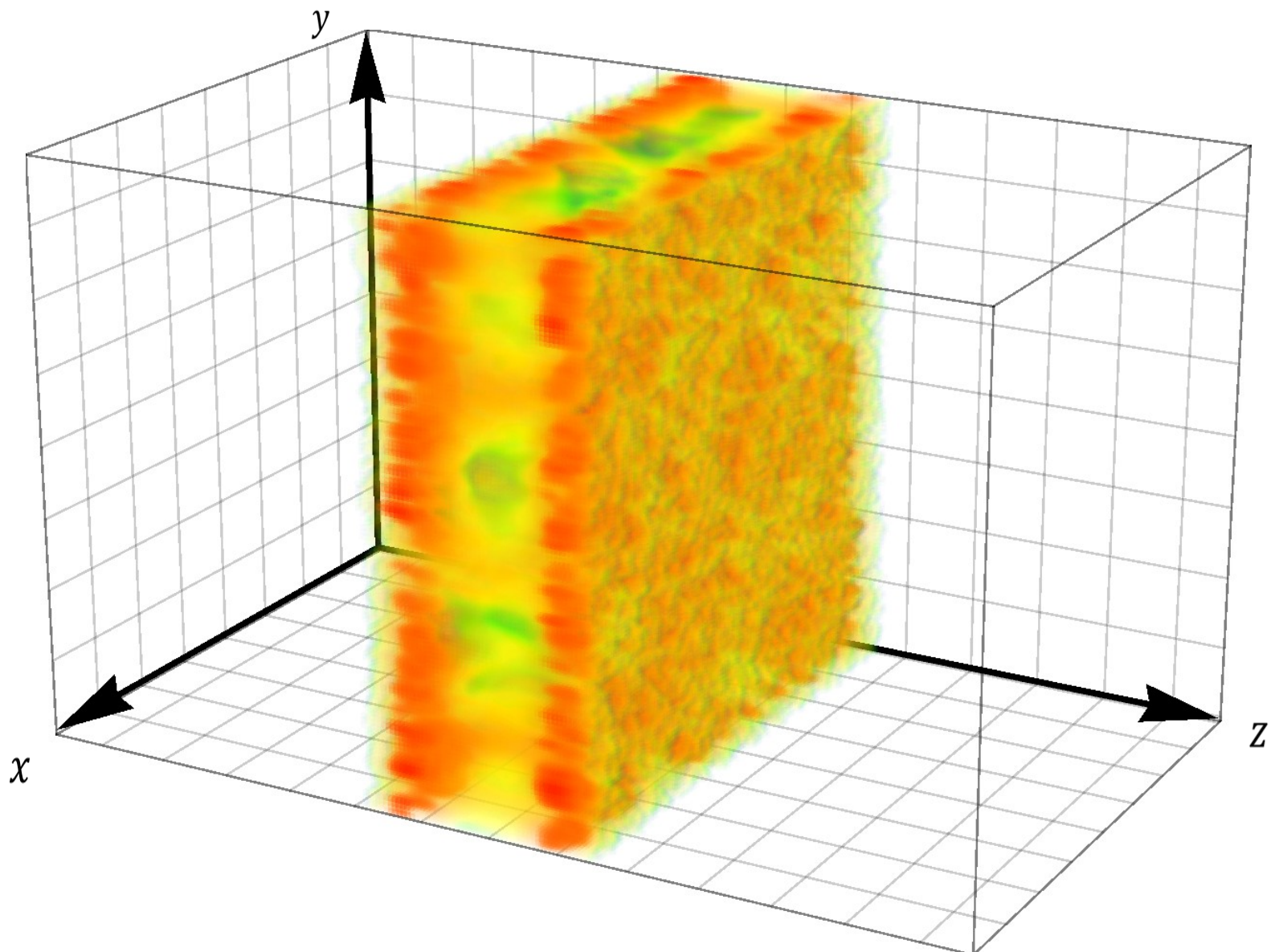
3D energy density



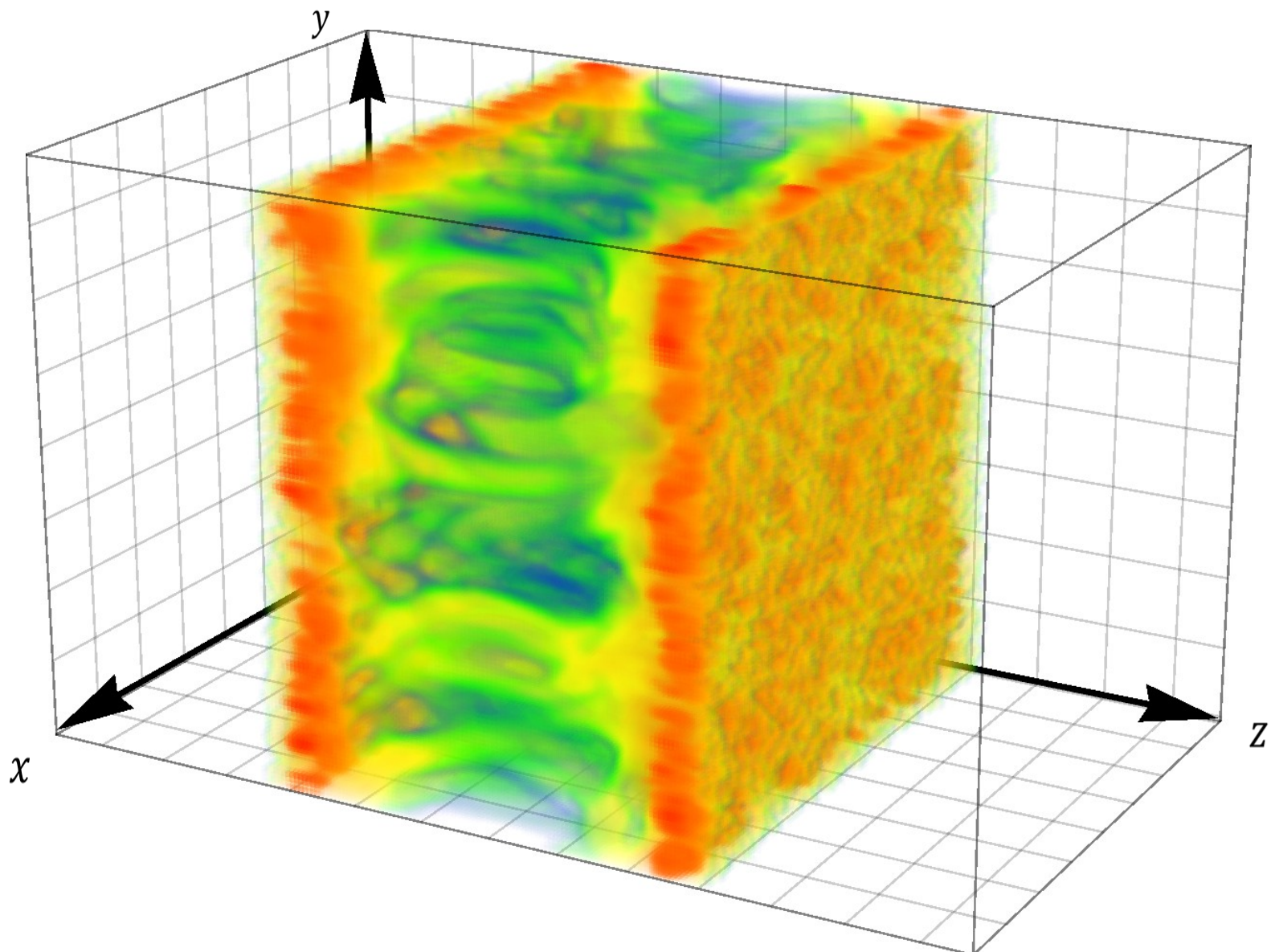
3D energy density



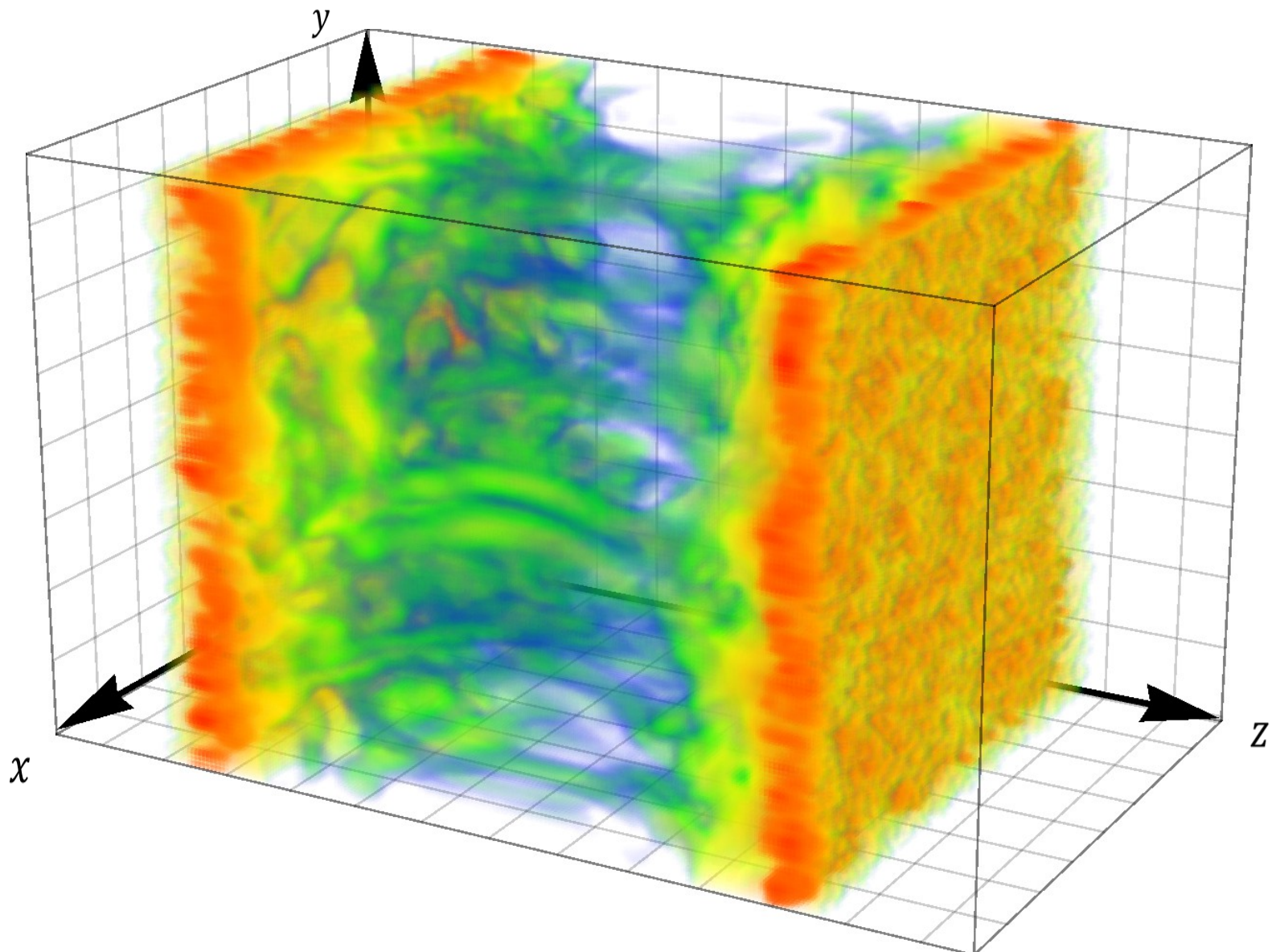
3D energy density



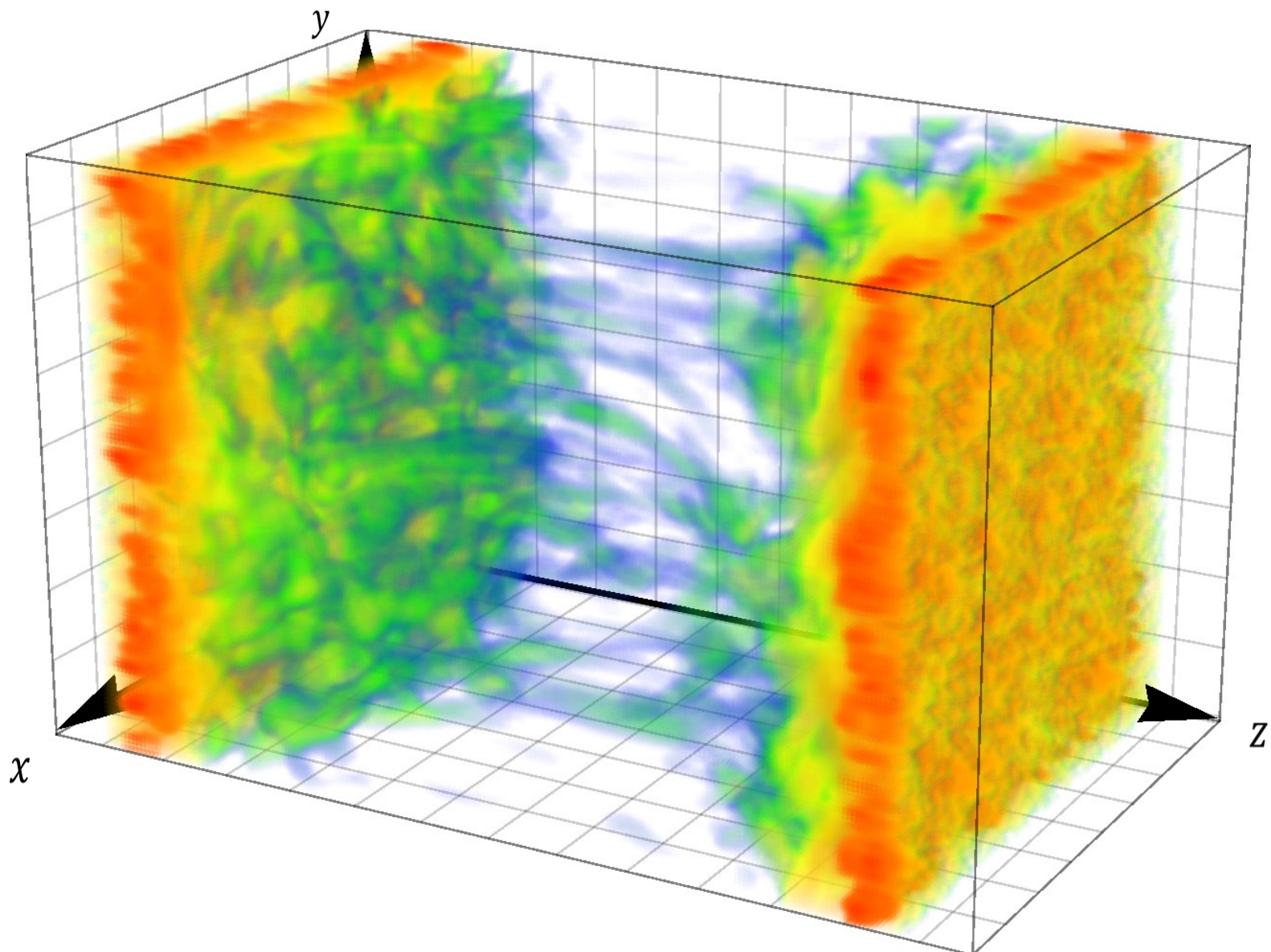
3D energy density



3D energy density

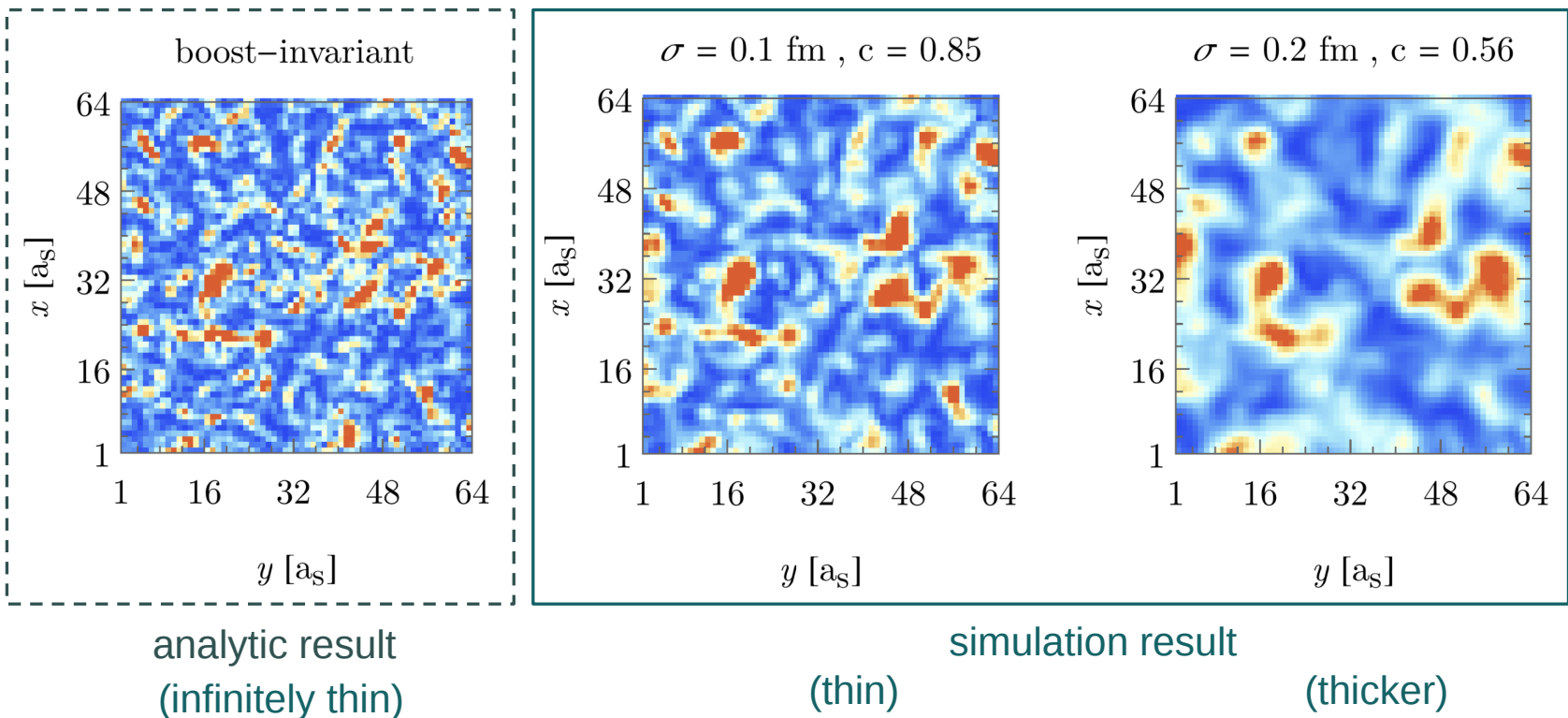


3D energy density



Comparison to boost-invariant results

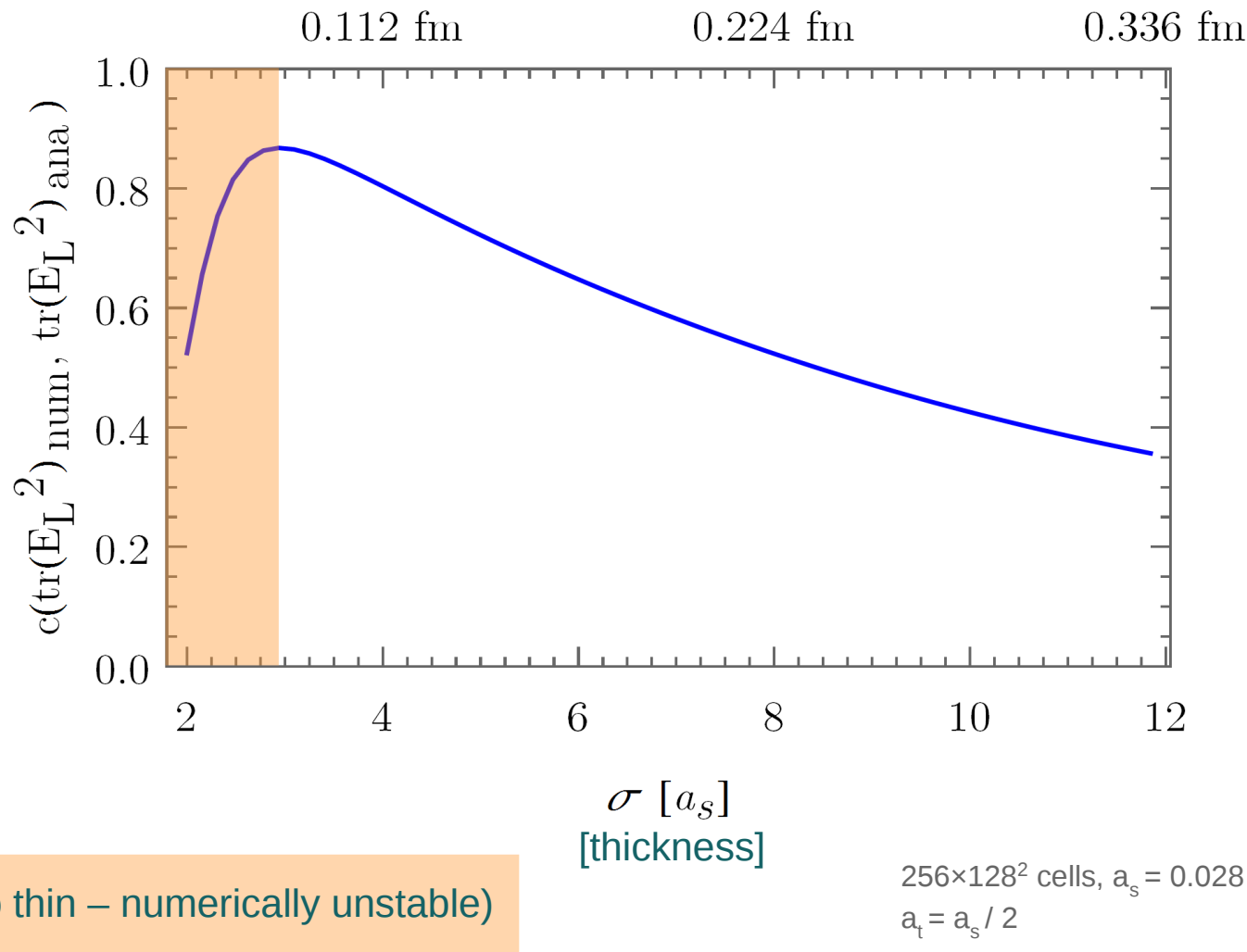
Energy density component $\text{tr } E_L^2(x_T)$ in the transverse plane at $t = 0$.



Au-Au collision in the McLerran-Venugopalan (MV) model for SU(2)

256×128^2 cells, $a_s = 0.028 \text{ fm}$
Shown: 64×64 cells

Correlation analytic \leftrightarrow numerical



Observables

Main observable: energy-momentum tensor $T^{\mu\nu}(x)$

- Build $T^{\mu\nu}(x)$ from electric and magnetic fields $E_i^a(x), B_i^a(x)$
- Average over configurations and integrate over transverse plane

$$\langle T^{\mu\nu} \rangle = \begin{pmatrix} \langle \varepsilon \rangle & 0 & 0 & \langle S_L \rangle \\ 0 & \langle p_T \rangle & 0 & 0 \\ 0 & 0 & \langle p_T \rangle & 0 \\ \langle S_L \rangle & 0 & 0 & \langle p_L \rangle \end{pmatrix} \quad \begin{aligned} \langle \varepsilon \rangle &= \frac{1}{2} \langle E_T^2 + B_T^2 + E_L^2 + B_L^2 \rangle \\ \langle p_T \rangle &= \frac{1}{2} \langle E_L^2 + B_L^2 \rangle \\ \langle p_L \rangle &= \frac{1}{2} \langle E_T^2 + B_T^2 - E_L^2 - B_L^2 \rangle \\ \langle S_L \rangle &= \left\langle (\vec{E}^a \times \vec{B}^a)_L \right\rangle \end{aligned}$$

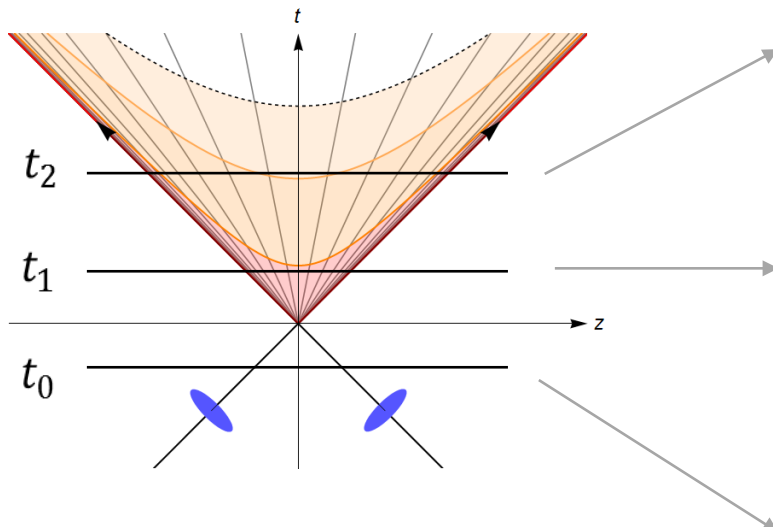
- Diagonalize, obtain local rest-frame energy density

$$\langle \varepsilon_{\text{loc}} \rangle = \frac{1}{2} \left(\langle \varepsilon \rangle - \langle p_L \rangle + \sqrt{(\langle \varepsilon \rangle + \langle p_L \rangle)^2 - 4 \langle S_L \rangle^2} \right)$$

Pressure anisotropy

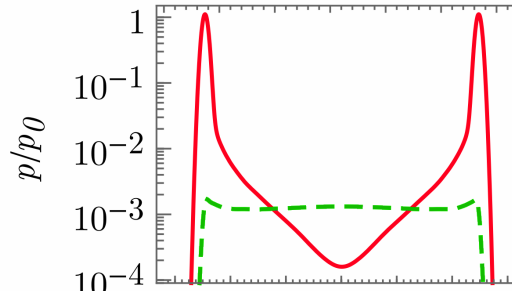
Longitudinal pressure $p_L(z)$ and transverse pressure $p_T(z)$

→ Pronounced pressure anisotropy

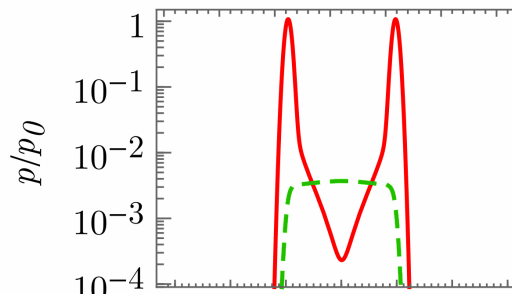


$$\langle p_T \rangle = \frac{1}{2} \langle E_L^2 + B_L^2 \rangle$$

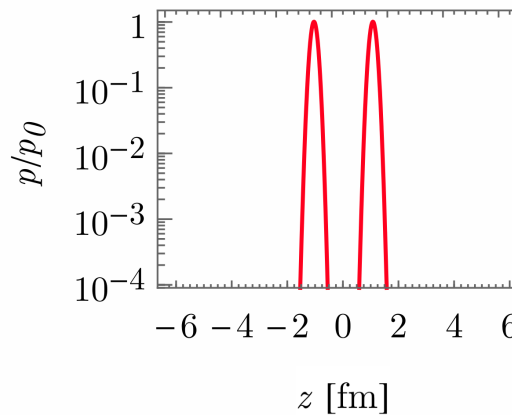
$$\langle p_L \rangle = \frac{1}{2} \langle E_T^2 + B_T^2 - E_L^2 - B_L^2 \rangle$$



$t_2 = +5 \text{ fm}/c$
(late times)



$t_1 = +2 \text{ fm}/c$
(after collision)

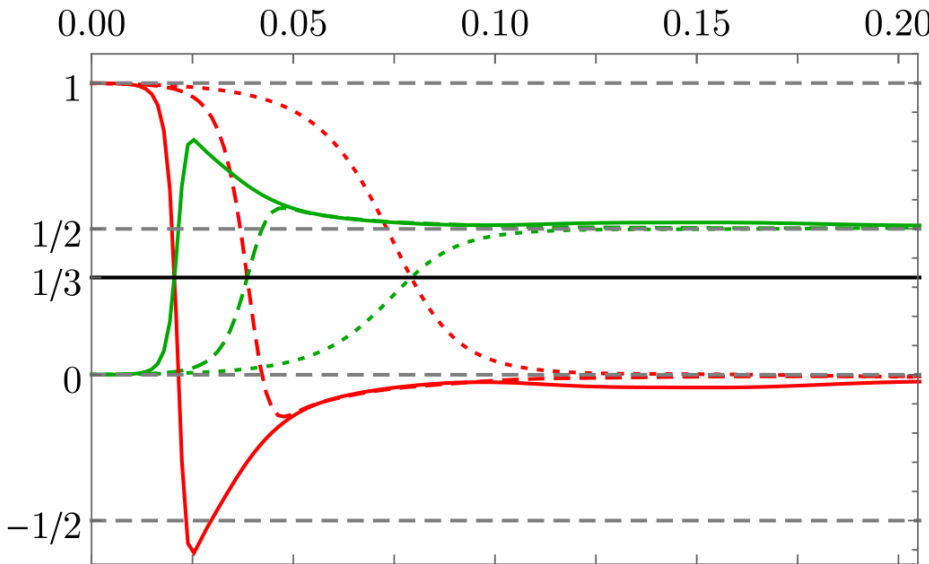


$t_0 = -1 \text{ fm}/c$
(before collision)

Pressure anisotropy at midrapidity

“Thin” nuclei ($\gamma \sim 200 - 1000$)

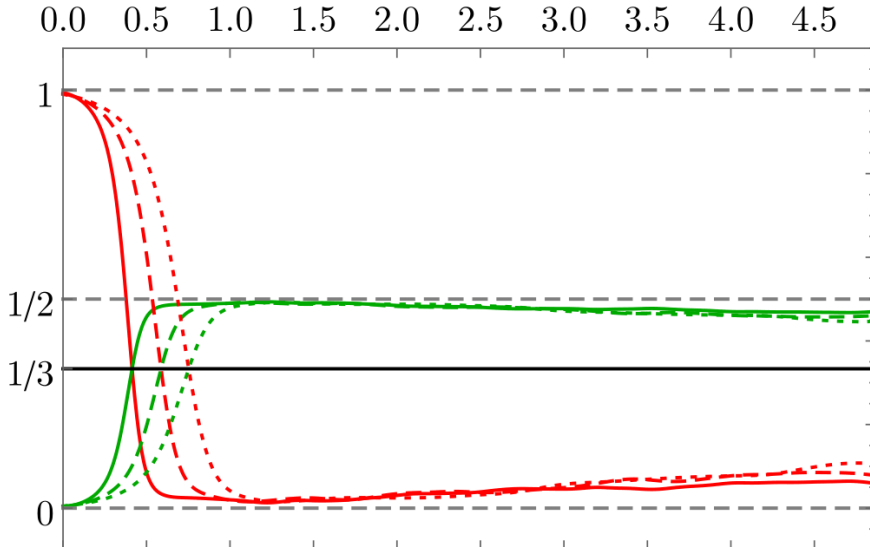
t [fm/c]



— $\sigma=0.008\text{fm}$ - - - $\sigma=0.016\text{fm}$... $\sigma=0.032\text{fm}$
— p_L/ϵ — p_T/ϵ

“Thick” nuclei ($\gamma \sim 20 - 40$)

t [fm/c]



— $\sigma=0.16\text{fm}$ - - - $\sigma=0.24\text{fm}$... $\sigma=0.32\text{fm}$
— p_L/ϵ — p_T/ϵ

observe very slow isotropization

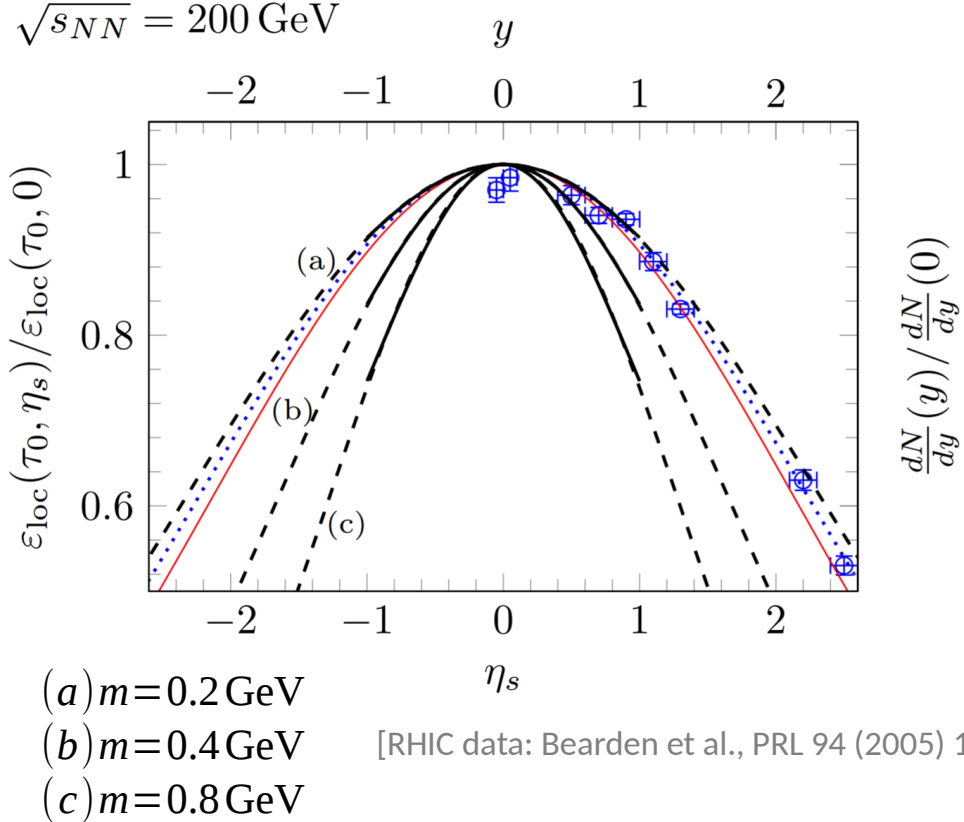
longitudinal pressure $p_L(z)$
transverse pressure $p_T(z)$

Rapidity profiles

Plot (space-time) rapidity profile of local rest-frame energy density

Compare to measured **rapidity profile of particle multiplicity (RHIC)** and **Landau model** prediction

$$\sqrt{s_{NN}} = 200 \text{ GeV}$$



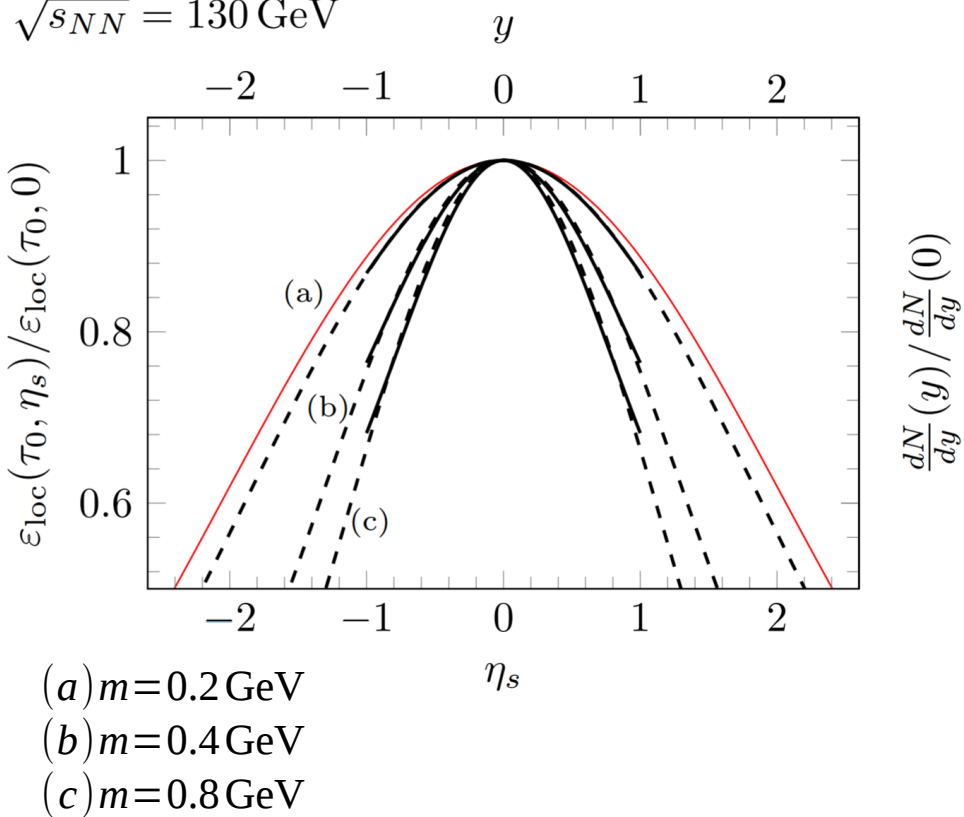
- Simulation data in interval $\eta_s \in (-1, 1)$ at $\tau = 1 \text{ fm}/c$
- Fit to Gaussian profile (dashed)
- Dependency on thickness (or rather \sqrt{s})
- Strong dependency on IR regulator, but $m=0.2 \text{ GeV}$ gives realistic shape
- However: no hydrodynamic expansion included
- Limited rapidity interval

Rapidity profiles

Plot (space-time) rapidity profile of local rest-frame energy density

Compare to measured **rapidity profile of particle multiplicity (RHIC)** and **Landau model** prediction

$$\sqrt{s_{NN}} = 130 \text{ GeV}$$

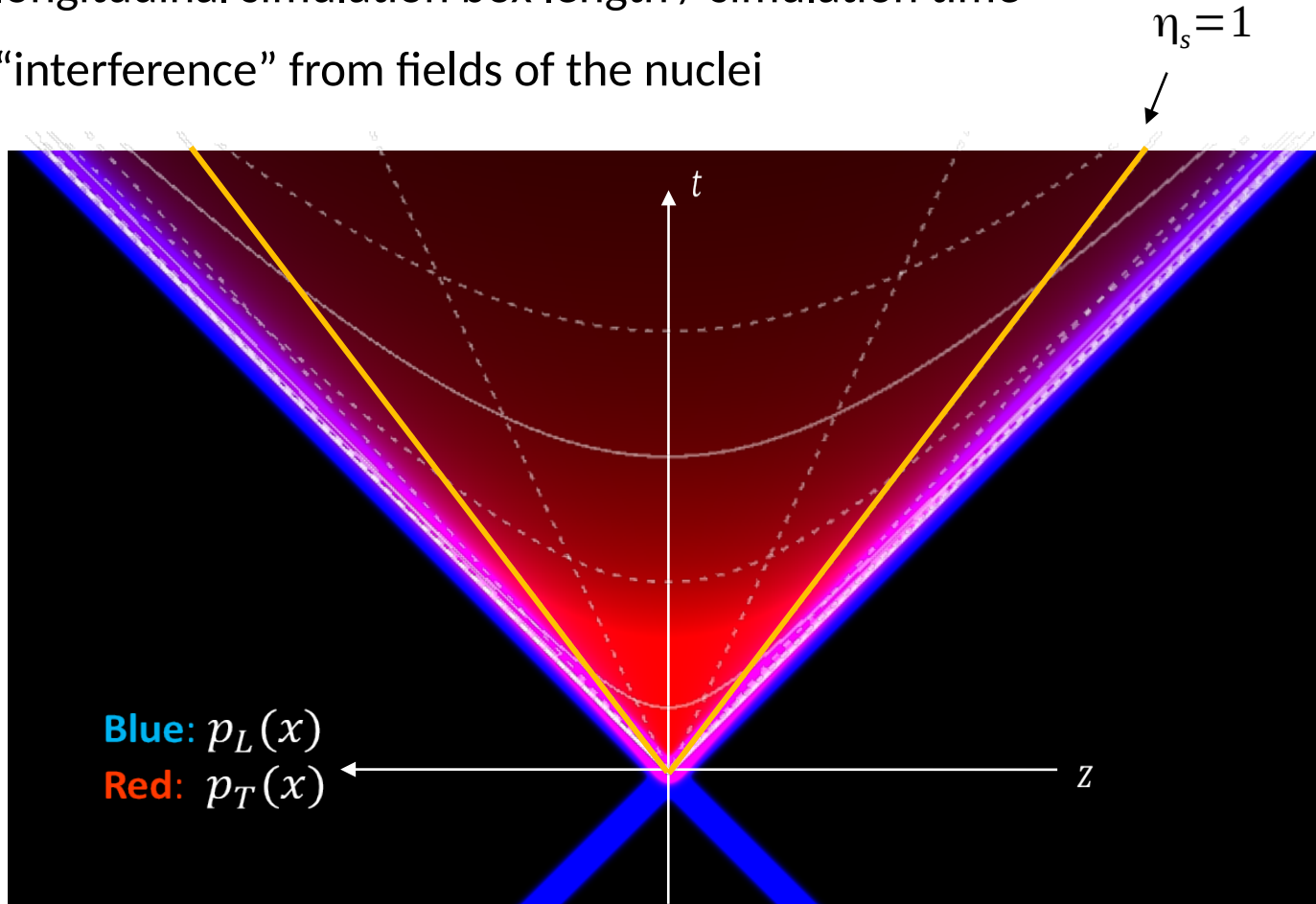


- Simulation data in interval $\eta_s \in (-1, 1)$ at $\tau = 1 \text{ fm}/c$
- Fit to Gaussian profile (dashed)
- Dependency on thickness (or rather \sqrt{s})
- Strong dependency on IR regulator, but $m=0.2 \text{ GeV}$ gives realistic shape
- However: no hydrodynamic expansion included
- Limited rapidity interval

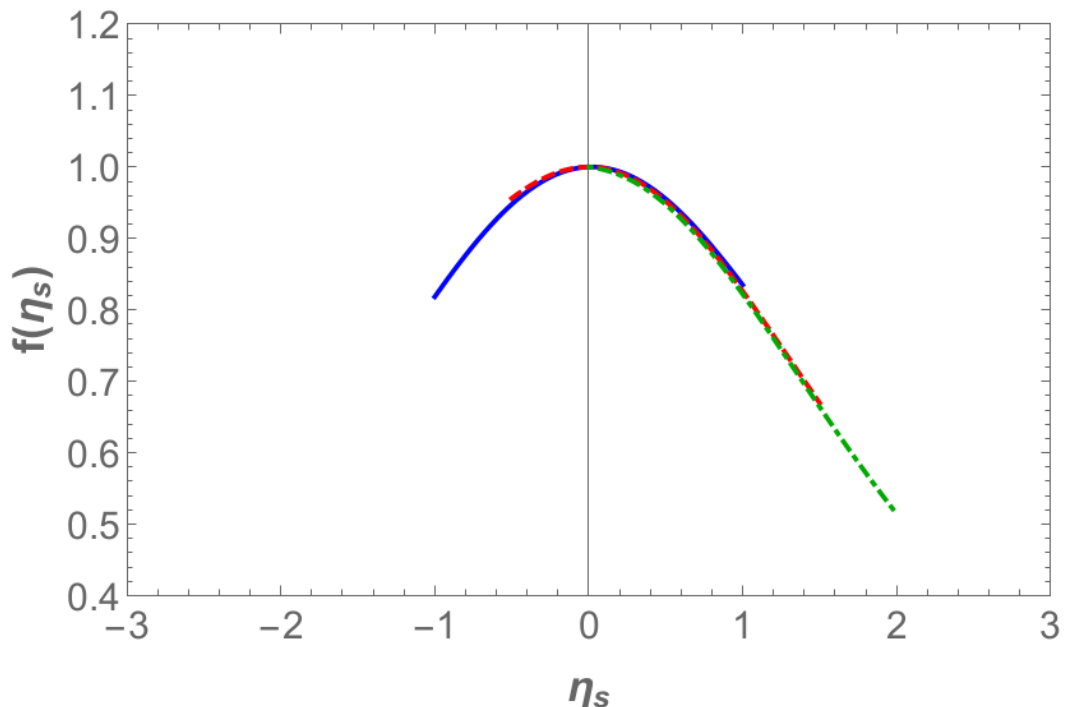
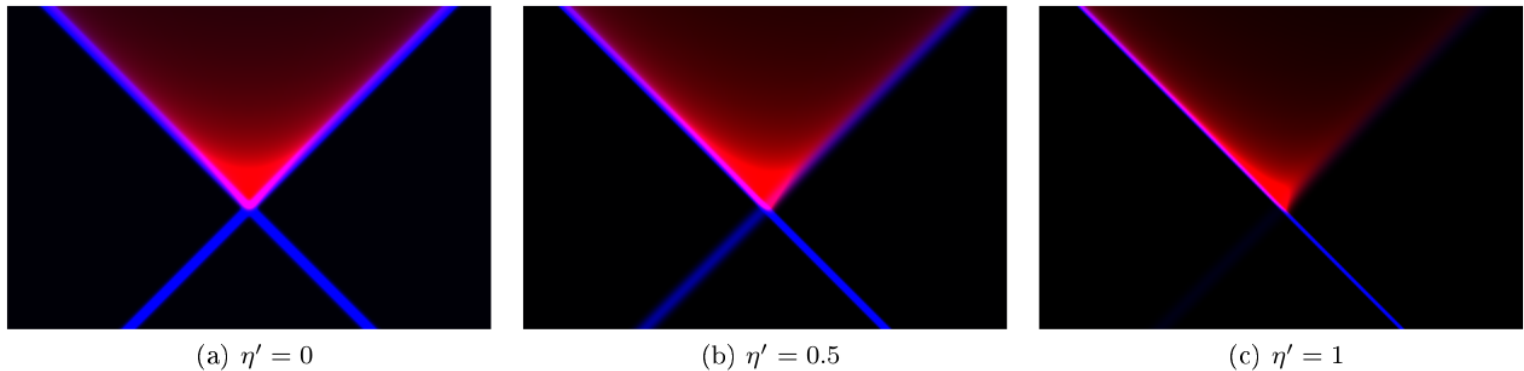
Rapidity profiles

Limited rapidity interval due to ..

- longitudinal simulation box length / simulation time
- “interference” from fields of the nuclei



Rapidity profiles

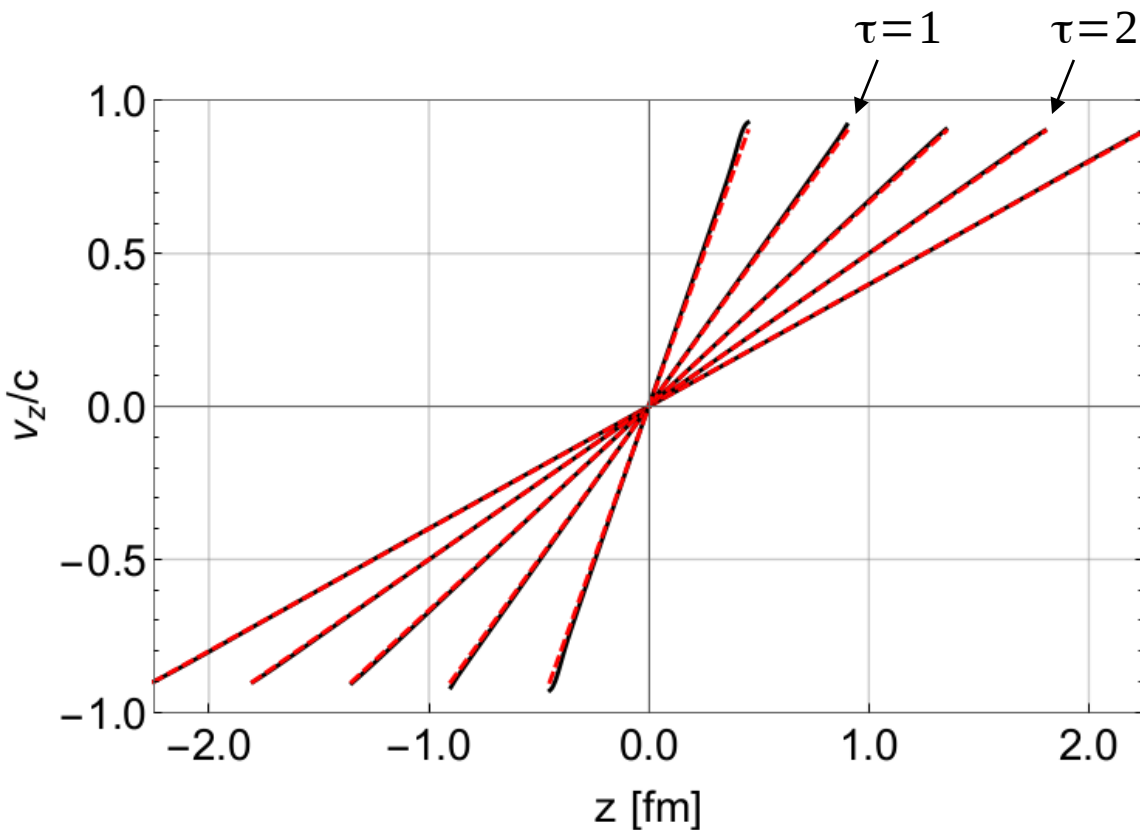


Combined rapidity profile
for increasingly boosted
collisions

Z

preliminary

Free streaming glasma



Compare local velocity
of glasma to free streaming
condition $v=z/t$

Lines (almost) on top of each
other.

Black solid: measured v_z

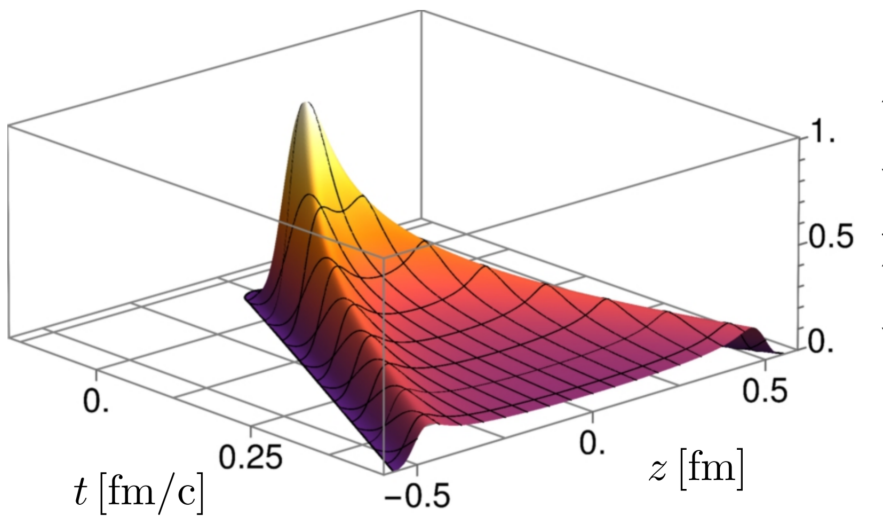
Red dashed: free streaming $v_{fs} = z/t$

Transverse pressure distribution

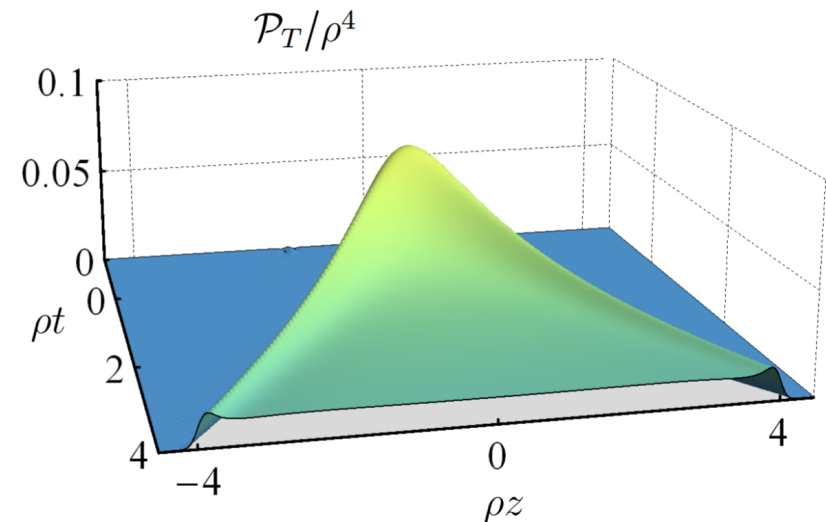
- Transverse pressure $p_T(x)$ generated by longitudinal fields

$$\langle p_T \rangle = \frac{1}{2} \langle E_L^2 + B_L^2 \rangle$$

- **Boost-invariant case:** initial conditions at $\tau=0$ for longitudinal E and B fields, i.e. constant p_T along the boundary of the forward light cone



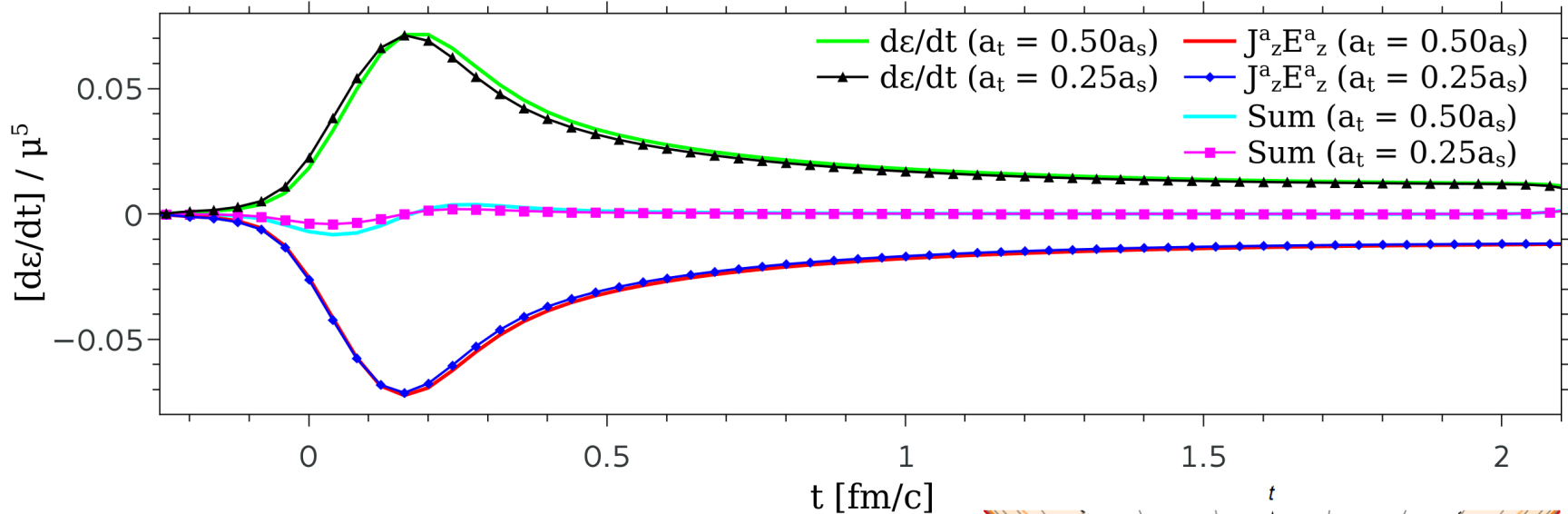
3+1 Yang-Mills



Holographic model

[Casalderrey-Solana et al., PRL (2013) 181601]

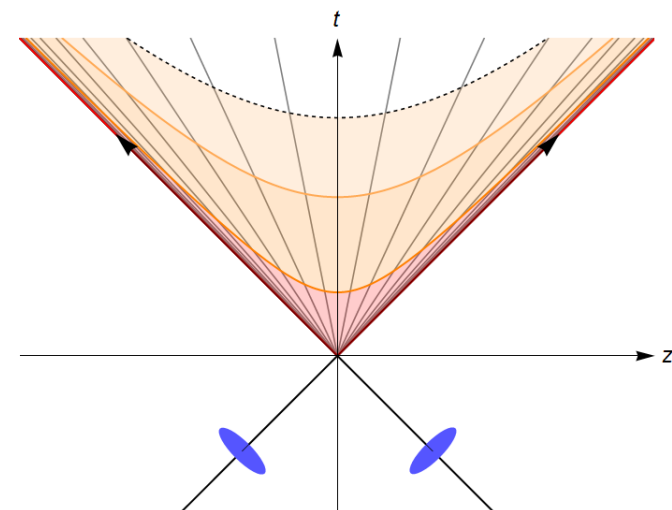
Energy production



Non-Abelian version of Poynting theorem

$$\frac{d\epsilon}{dt} + \frac{1}{V} \int \partial_i S_i d^3x + \frac{1}{V} \int E_i^a J_i^a d^3x = 0$$

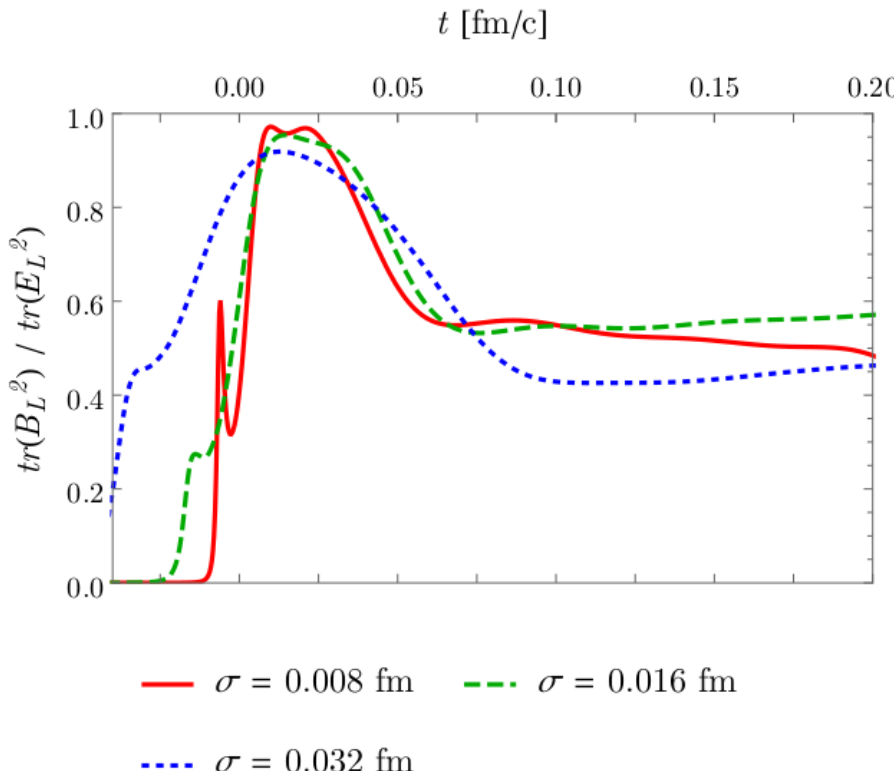
Energy production caused by longitudinal chromoelectric fields



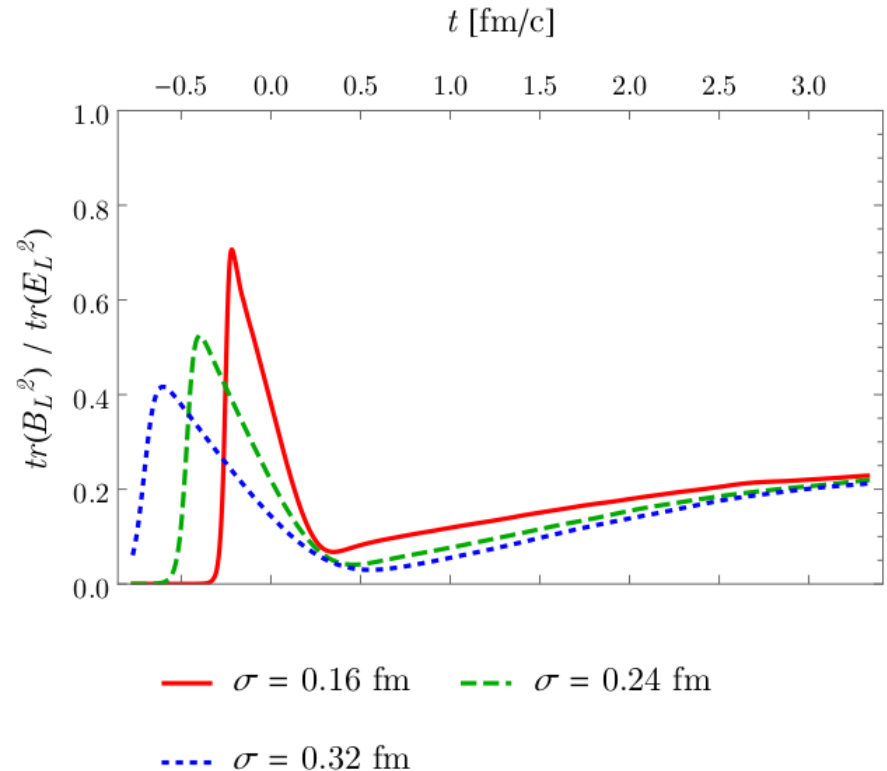
Chromo-magnetic suppression?

Ratio of longitudinal magnetic over longitudinal electric contributions

“Thin” nuclei ($\gamma \sim 200 - 1000$)



“Thick” nuclei ($\gamma \sim 20 - 40$)

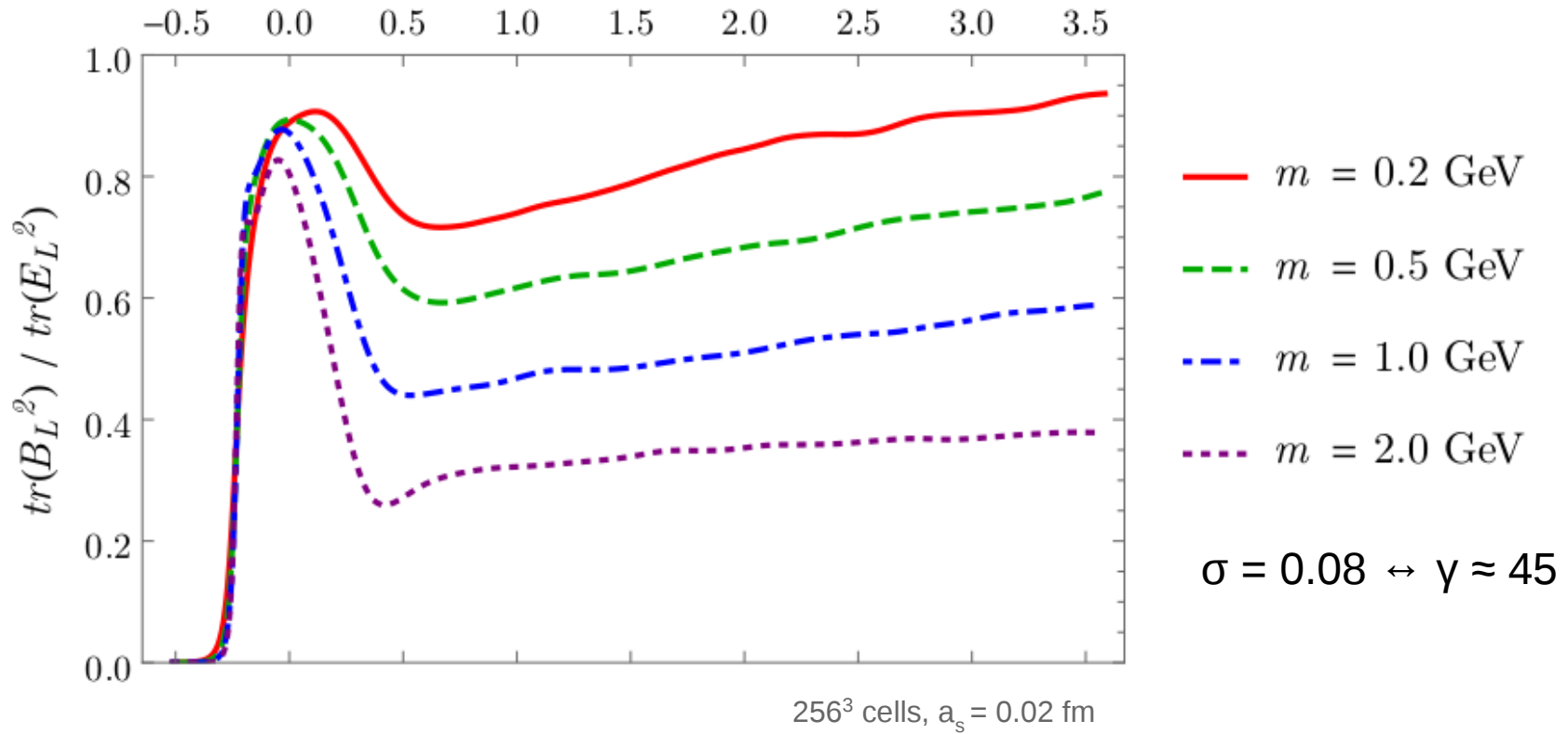


Small ratio for thick nuclei

Chromo-magnetic suppression?

Ratio of longitudinal magnetic over longitudinal electric contributions

t [fm/c]

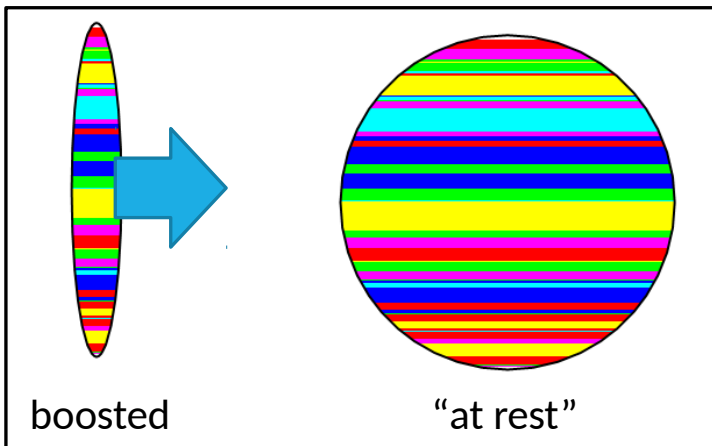


Strong dependence on IR regulator m

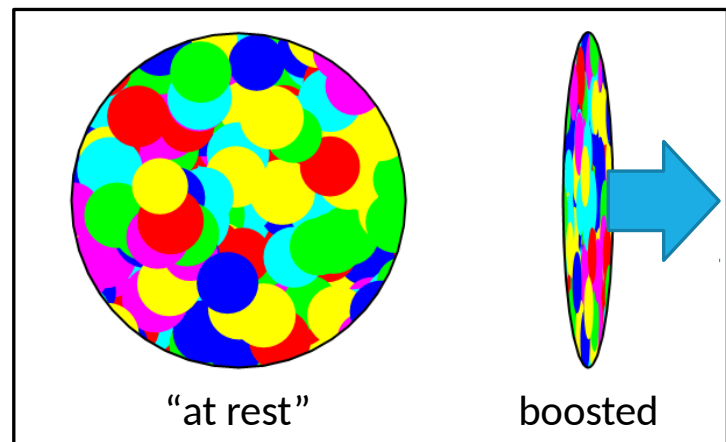
→ spurious effect of our choice of initial conditions?

Longitudinal structure

Current implementation



Longitudinal randomness



Longitudinal randomness...

- leads to higher energy density in the plasma
[Fukushima, PRD 77 (2008) 074005]
- could provide boost-invariance breaking perturbations, which can drive system towards isotropization
[Epelbaum, Gelis, PRL 111 (2013) 232301]

Longitudinal structure

Wilson line expectation value $\langle \text{tr}(V) \rangle$ of a single nucleus is sensitive to longitudinal structure.

Embedded 2D MV-model:

$$\langle \hat{\rho}^a(\mathbf{x}_T) \hat{\rho}^b(\mathbf{x}'_T) \rangle = g^2 \mu^2 \delta^{(2)}(\mathbf{x}_T - \mathbf{x}'_T) \delta^{ab}$$

$$\rho(t, z, \mathbf{x}_T) = f(z-t) \hat{\rho}(\mathbf{x}_T)$$

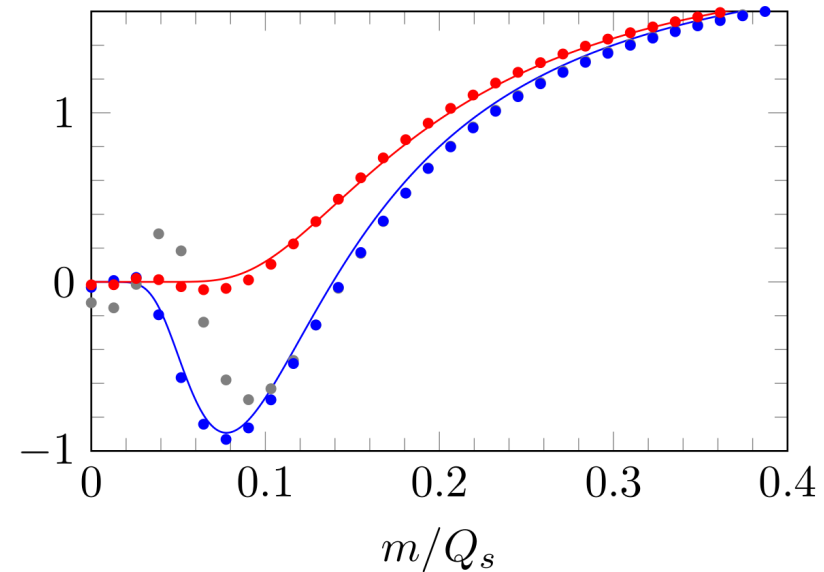
3D MV-model:

(with random longitudinal structure)

$$\langle \rho^a(x^-, \mathbf{x}) \rho^b(x^-, \mathbf{x}') \rangle = g^2 \mu^2 f(x^-) \delta(x^- - x'^-) \delta^{(2)}(\mathbf{x}_T - \mathbf{x}'_T) \delta^{ab}$$

$$f(z) \dots \text{longitudinal profile function} \quad x^- = \frac{t-z}{\sqrt{2}}$$

Introducing independent “sheets” in longitudinal direction
[Fukushima, PRD 77 (2008) 074005]



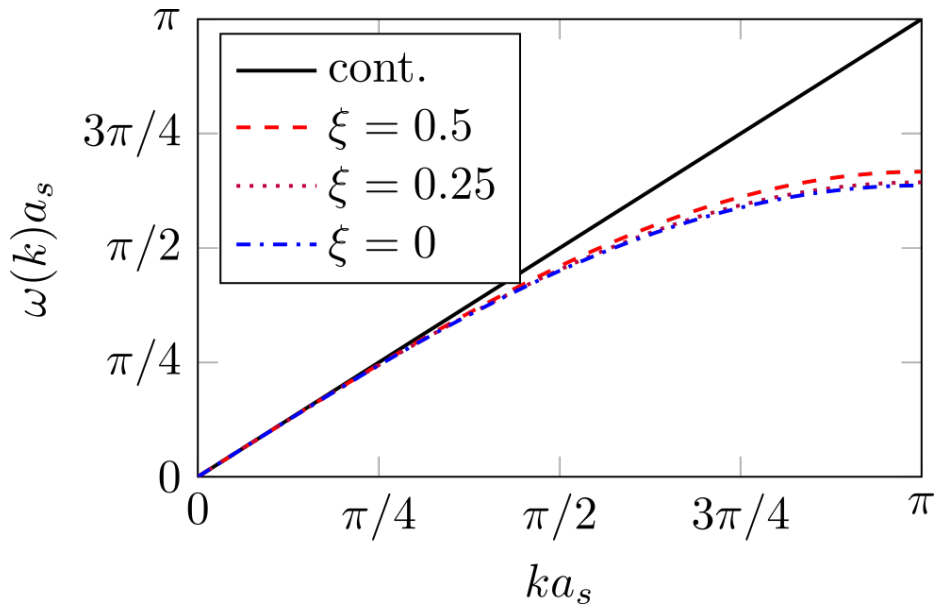
Lines: analytical result
Dots: numerical result

Blue: 2D MV-model
Red: 3D MV-model
Gray: intermediate

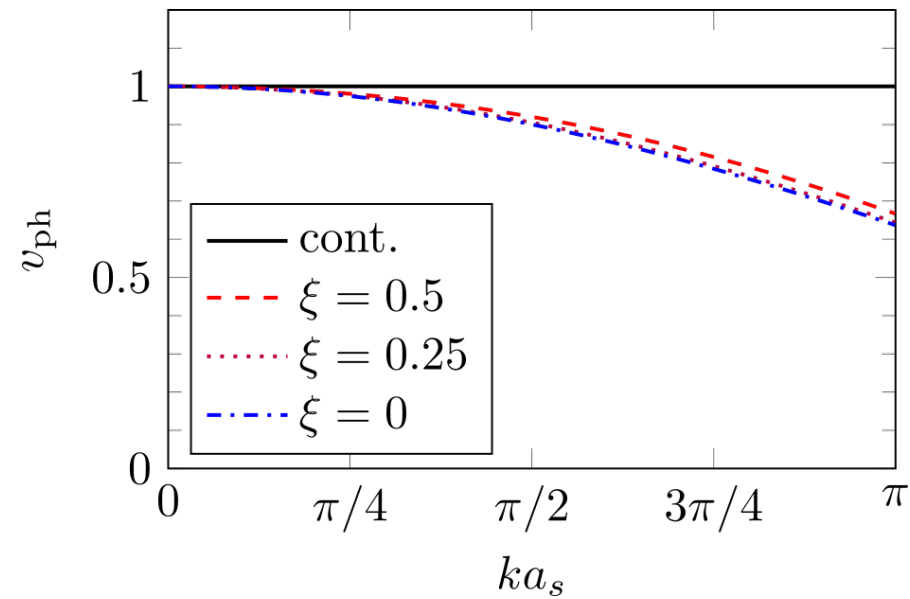
preliminary

Lattice dispersion

Dispersion relation



Phase velocity



Temporal to spatial lattice spacing: $\xi = \frac{a_t}{a_s}$

Courant-Friedrichs-Lowy (CFL) condition: $\xi \leq \frac{1}{\sqrt{d}}$ in d dimensions
(for explicit solvers like the Leapfrog algorithm)

Explicit vs. implicit solvers

Continuum action: $S[\phi] = \frac{1}{2} \int_x \partial_\mu \phi \partial^\mu \phi$ 1D scalar field example

Equations of motion : $\delta S = 0 \Rightarrow \partial_\mu \partial^\mu \phi = \partial_t^2 \phi - \partial_x^2 \phi = 0$

Discretized: $\frac{\phi(x, t+1) - 2\phi(x, t) + \phi(x, t-1)}{a_t} = \frac{\phi(x+1, t) - 2\phi(x, t) + \phi(x-1, t)}{a_s}$

Explicit solver: $\phi(x, t+1) = F(\phi(\dots, t), \phi(\dots, t-1))$

Implicit solver: $\phi(x, t+1) = F(\phi(\dots, t+1), \phi(\dots, t), \phi(\dots, t-1))$

Discretized action for explicit solver:

$$S[\phi] = \frac{1}{2} V \sum_x \left\{ \left(\frac{\phi(x, t+1) - \phi(x, t)}{a_t} \right)^2 + \left(\frac{\phi(x+1, t) - \phi(x, t)}{a_s} \right)^2 \right\}$$

Variational integrators

Usual approach

Variation

$$\delta S = 0$$



Continuum

$$S[\phi] = \int d^4x \mathcal{L}(\phi(x), \partial_\mu \phi(x), \dots)$$

Equations of motion
+ preserved constraints

$$\partial_\mu \partial^\mu \phi(x) + \dots = 0$$

$$C(\phi(x)) = 0$$



Variational integrators

Discretization
(finite differences,
sums, ...)

Discretized action

$$S[\phi] = V \sum_x \mathcal{L}(\phi_x, \bar{\partial}_\mu \phi_x, \dots)$$

If possible: keep symmetries!

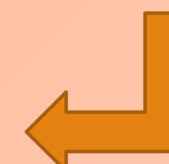
Discretization
(finite differences,
sums, ...)



Discretized equations
of motion + constraints (?)

$$\bar{\partial}_\mu \bar{\partial}^\mu \phi(x) + \dots = 0$$

$$\bar{C}(\phi_x) = 0$$

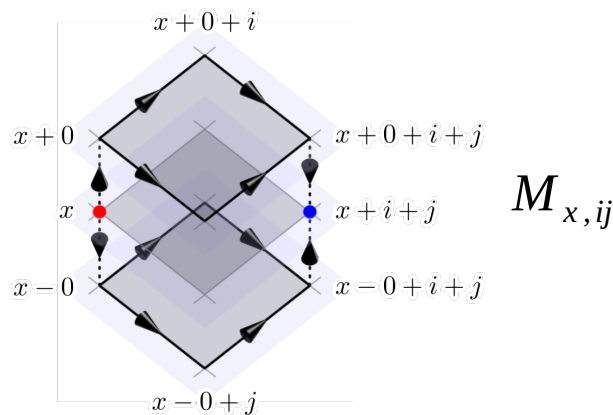
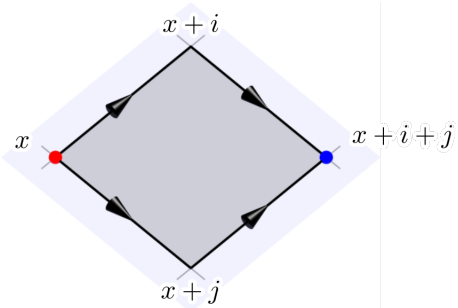
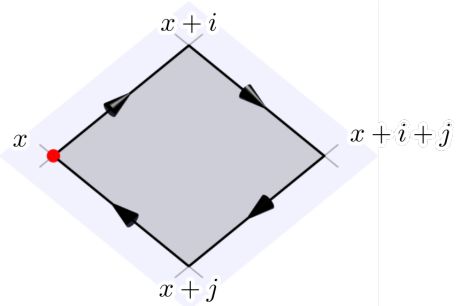


Discrete Variation

$$\delta S = 0$$

"Inherited" symmetries

Lattice gauge theory



Link variable: $U_{x,\mu} \simeq \exp(i g a^\mu A_{x,\mu})$

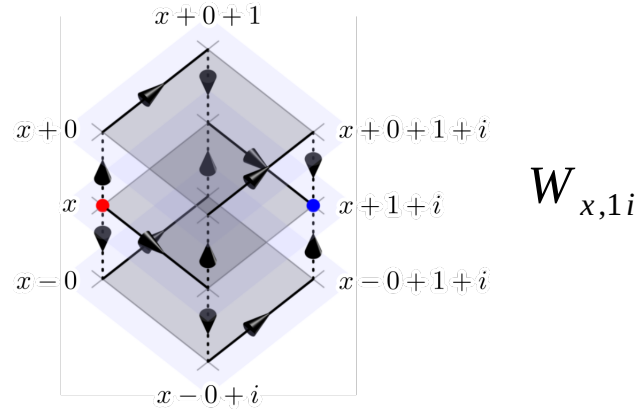
Plaquette: $U_{x,\mu\nu} = U_{x,\mu} U_{x+\mu,\nu} U_{x+\mu+\nu,-\mu} U_{x+\nu,-\mu}$

Relation to field strength tensor:

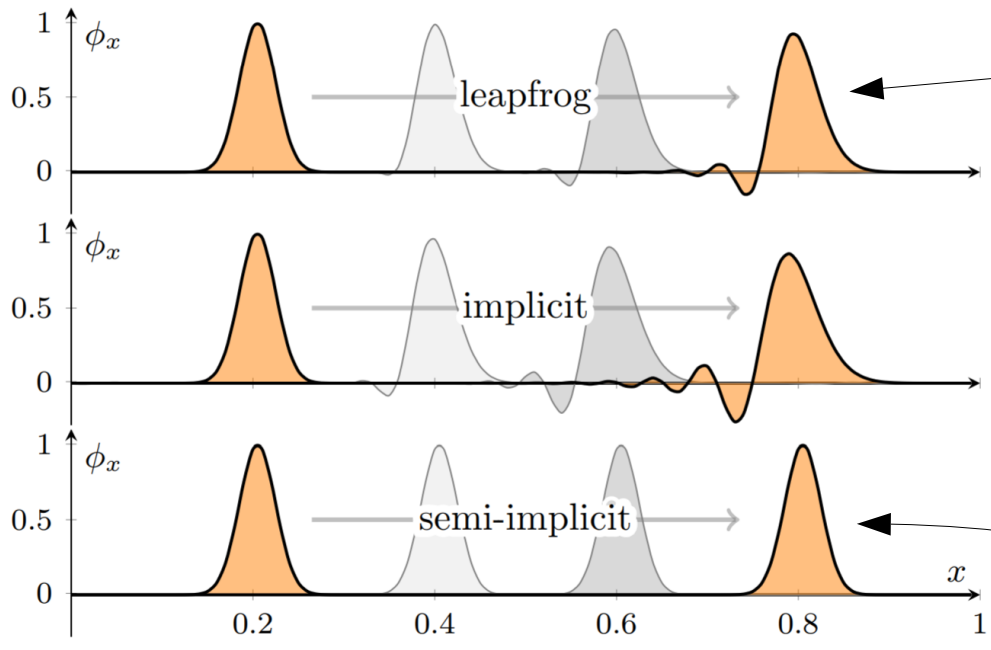
$$\text{tr}(2 - U_{x,\mu\nu} - U_{x,\mu\nu}^\dagger) \simeq \frac{1}{2} \sum_a (g a^\mu a^\nu F_{\mu\nu}^a(x))^2$$

$$C_{x,\mu\nu} \equiv U_{x,\mu} U_{x+\mu,\nu} - U_{x,\nu} U_{x+\nu,\mu}$$

$$\text{Identity: } C_{x,\mu\nu} C_{x,\mu\nu}^\dagger = 2 - U_{x,\mu\nu} - U_{x,\mu\nu}^\dagger$$



Dispersion-free propagation



Standard Wilson action:

$$S[U] = \frac{V}{g^2} \sum_x \left(\sum_i \frac{1}{(a^0 a^i)^2} \text{tr} \left(2 - U_{x,0i} - U_{x,0i}^\dagger \right) - \frac{1}{2} \sum_{i,j} \frac{1}{(a^i a^j)^2} \text{tr} \left(2 - U_{x,ij} - U_{x,ij}^\dagger \right) \right)$$

Discretized action for the **semi-implicit scheme**:

$$S[U] = \frac{V}{g^2} \sum_x \left(\frac{1}{(a^0 a^1)^2} \text{tr} \left(C_{x,01} C_{x,01}^\dagger \right) + \sum_i \frac{1}{(a^0 a^i)^2} \text{tr} \left(C_{x,0i} C_{x,0i}^\dagger \right) - \frac{1}{4} \sum_{i,|j|} \frac{1}{(a^i a^j)^2} \text{tr} \left(C_{x,ij} M_{x,ij}^\dagger \right) - \frac{1}{4} \sum_{|j|} \frac{1}{(a^1 a^j)^2} \text{tr} \left(C_{x,1j} W_{x,1j}^\dagger + \text{h.c.} \right) \right)$$

implicit part

semi-implicit part

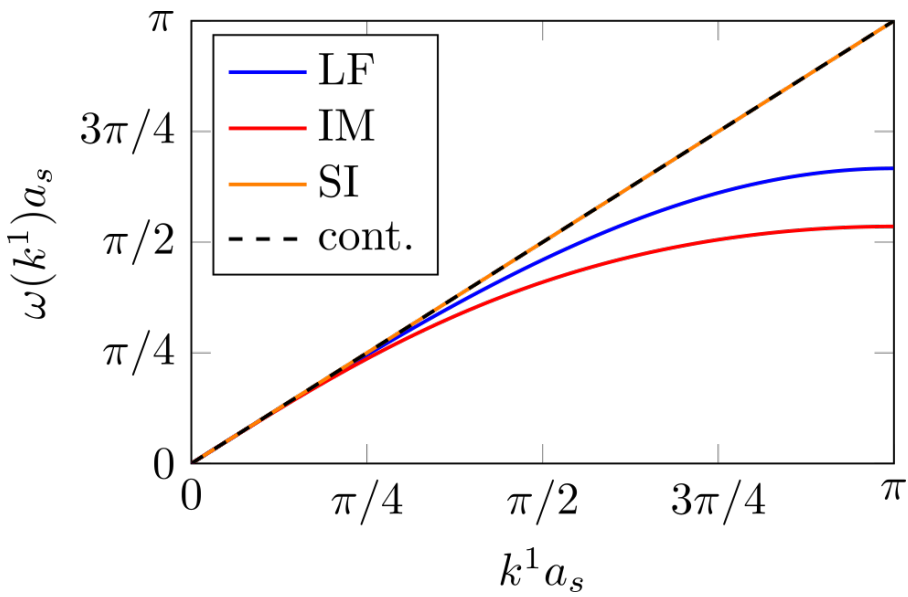
with $C_{x,\mu\nu} \equiv U_{x,\mu} U_{x+\mu,\nu} - U_{x,\nu} U_{x+\nu,\mu}$ etc.

Variational integrator:
Discretized equations of motion from discretized action

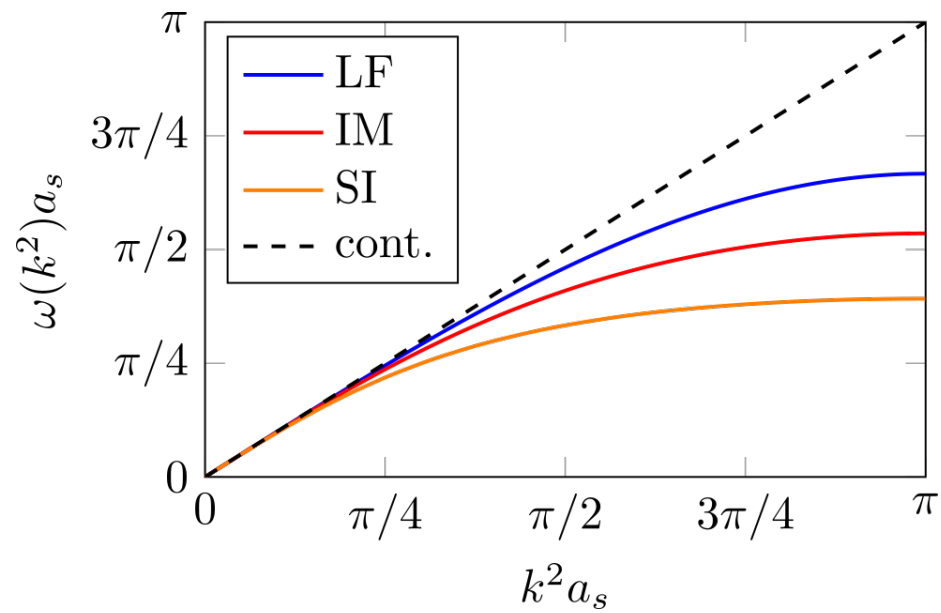
For details see:
Al, D. Müller, Eur.Phys.J.
C78 (2018) no.11, 884

Lattice dispersion

Longitudinal direction

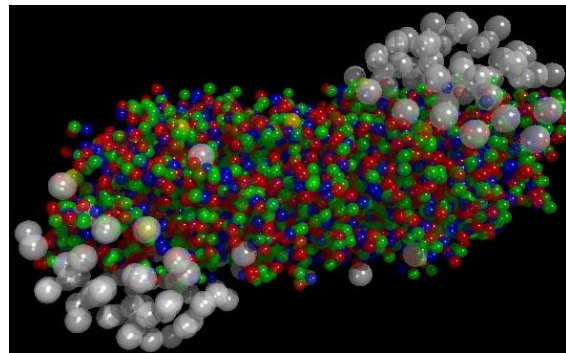
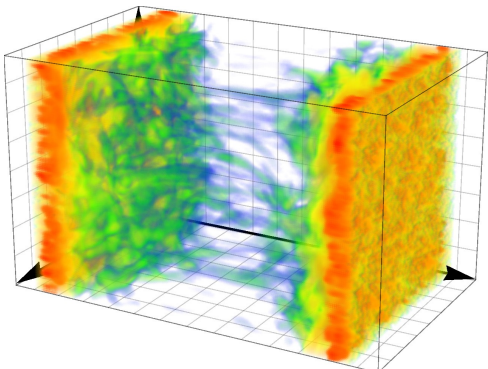


Transverse direction



Lattice dispersion for leapfrog (LF), implicit (IM) and semi-implicit (SI) schemes.

Computational challenges



Simulating small part of nuclei
at RHIC energies:

γ -factor: 100
Lattice: 2048×192^2 cells
Gauge group: SU(2)
Color sheets: 1
Simulation box: $(6 \text{ fm})^3$

- **25 GB** simulation data
- **192 core hours** on
Vienna Scientific Cluster (VSC-3)

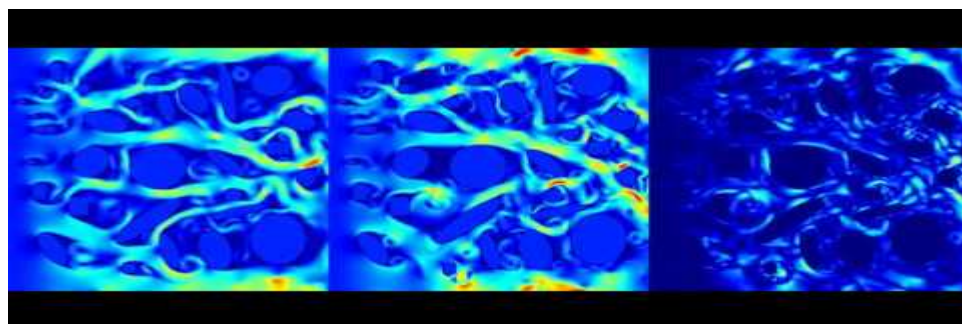
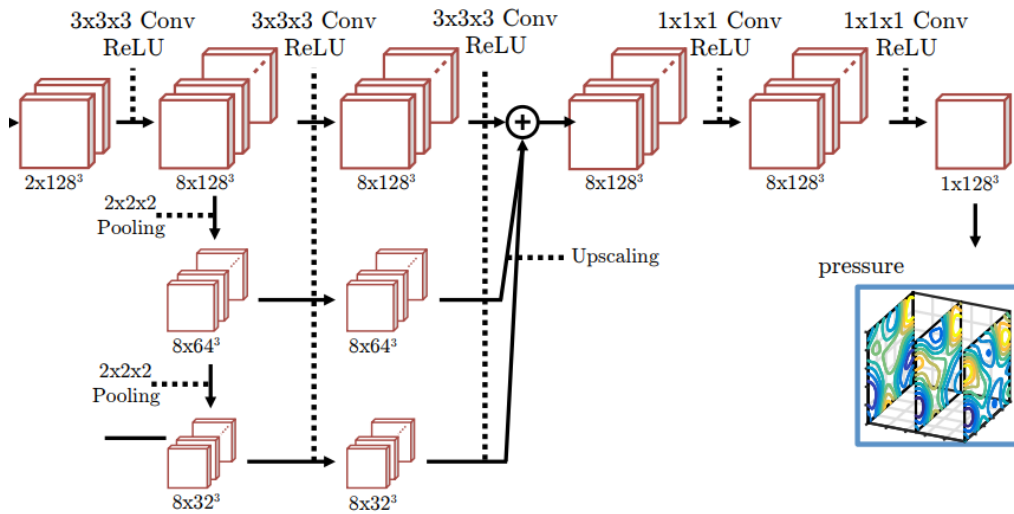
Simulating realistic off-central full size
nuclei at LHC energies:

γ -factor: 2500
Lattice: $(25 \times 20480) \times 1920^2$ cells
Gauge group: SU(3)
Color sheets: 100
Simulation box: $(60 \text{ fm})^3$

- **25 PB** simulation data
- **5 million core years** on VSC-3
(150 years on VSC3; but only 130 TB available)

Machine learning in fluid dynamics

Accelerating Eulerian Fluid Simulation With Convolutional Networks
Tompson et al, arxiv:1607.03597

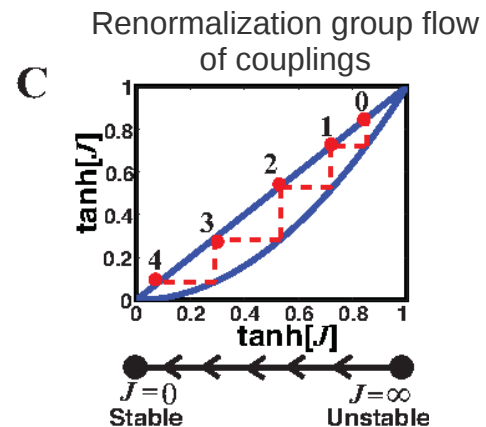
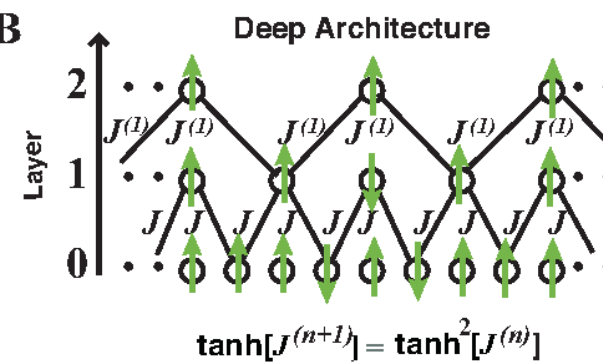
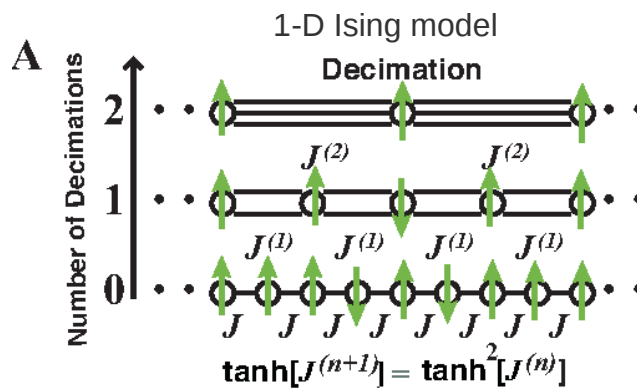


- Compress computation time and memory usage
- Use convolutional autoencoders to compress state size
- Learn dynamics on compressed form
- Can generalize to larger grid sizes

Lat-Net: Compressing Lattice Boltzmann Flow Simulations using Deep Neural Networks
Hennigh, arxiv:1705.09036

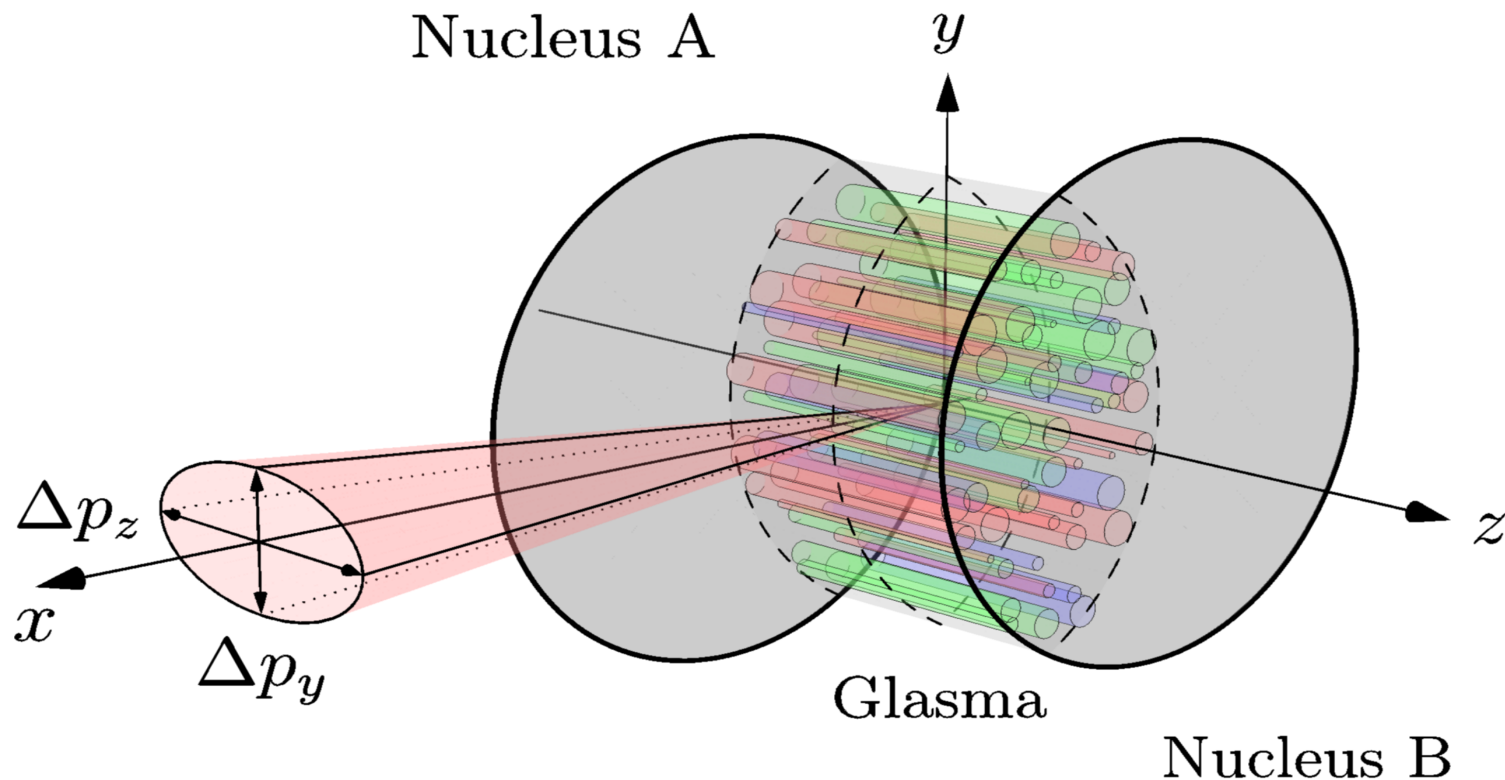
Beyond speeding up simulations...

- Why do neural networks work surprisingly well in some cases, and why and how can they fail in others?
 - we can compare to ground-truth physical result
- Learn about physical system from new viewpoint involving machine learning tools
 - latent space representation can capture relevant degrees of freedom
 - irrelevant degrees of freedom are integrated out into weight parameters
- Renormalization group picture of deep neural networks:



An exact mapping between the Variational Renormalization Group and Deep Learning
Mehta, Schwab, arxiv:1410.3831

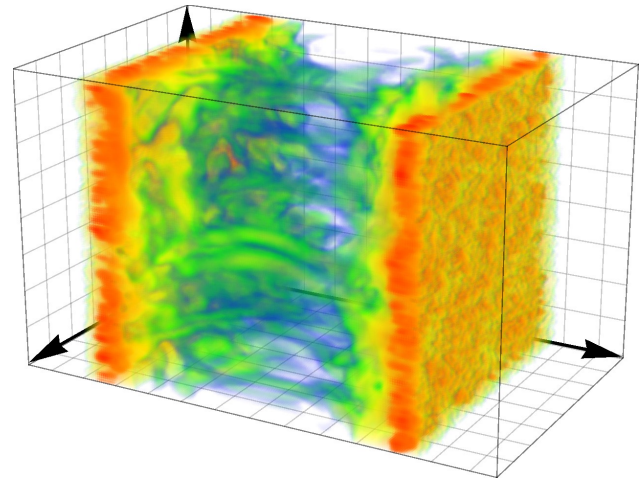
Jet momentum broadening



Work in preparation, together with Daniel Schuh and David Müller

Conclusions & Outlook

- Simulate CGC collisions in 3D+1 using Colored Particle-In-Cell
- Finite thickness breaks boost invariance → Gaussian rapidity profiles
- **Outlook:**
 - Study effect of random longitudinal structure
 - Observables at early times:
gluon production,
momentum broadening, ...
 - Explore machine learning



D. Gelfand, AI, D. Müller, Phys. Rev. D94 (2016) no.1, 014020
AI, D. Müller, Phys. Lett. B (2017) 771
AI, D. Müller, Eur.Phys.J. C78 (2018) no.11, 884

open source:
www.openpixi.org